EXHIBIT 77

JOURNAL OF NEUROTRAUMA 30:1299–1304 (July 15, 2013)
© Mary Ann Liebert, Inc.
DOI: 10.1089/neu.2012.2690

Short Communications

Profile of Self-Reported Problems with Executive Functioning in College and Professional Football Players

Daniel R. Seichepine,[1,2] Julie M. Stamm,[2] Daniel H. Daneshvar,[2] David O. Riley,[2] Christine M. Baugh,[2] Brandon E. Gavett,[3] Yorghos Tripodis,[4] Brett Martin,[5] Christine Chaisson,[5] Ann C. McKee, M.D.,[1,2,6–8] Robert C. Cantu,[2,9,10] Christopher J. Nowinski,[2] and Robert A. Stern[1,2,7,10]

Abstract

Repetitive mild traumatic brain injury (mTBI), such as that experienced by contact-sport athletes, has been associated with the development of chronic traumatic encephalopathy (CTE). Executive dysfunction is believed to be among the earliest symptoms of CTE, with these symptoms presenting in the fourth or fifth decade of life. The present study used a well-validated self-report measure to study executive functioning in football players, compared to healthy adults. Sixty-four college and professional football players were administered the Behavior Rating Inventory of Executive Function, adult version (BRIEF-A) to evaluate nine areas of executive functioning. Scores on the BRIEF-A were compared to published age-corrected normative scores for healthy adults Relative to healthy adults, the football players indicated significantly more problems overall and on seven of the nine clinical scales, including Inhibit, Shift, Emotional Control, Initiate, Working Memory, Plan/Organize, and Task Monitor. These symptoms were greater in athletes 40 and older, relative to younger players. In sum, football players reported more-frequent problems with executive functioning and these symptoms may develop or worsen in the fifth decade of life. The findings are in accord with a growing body of evidence that participation in football is associated with the development of cognitive changes and dementia as observed in CTE.

Key words: chronic traumatic encephalopathy; executive function; football; traumatic brain injury

Introduction

Traumatic brain injury (TBI) is a significant public health problem. It is estimated that approximately 1.7 million TBIs occur in the United States annually, resulting in emergency department visits, hospitalization, or death, with direct and indirect costs totaling approximately $76.5 billion a year.[1–3] Moderate to severe TBI (sTBI) is associated with a wide range of long-term cognitive deficits.[4] Though early research focused on the effects of moderate to sTBI, attention has increasingly turned to the long-term consequences of repetitive mild TBI (mTBI), such as that experienced by contact-sport athletes. It has been estimated that 1.6–3.8 million sport-related mTBIs occur annually,[5,6] with the greatest number occurring in football.[7,8] With over 60 million youth and adolescents participating in organized sports each year, a number that increased by 16 million from 1997 to 2008, sport-related TBI is an important and growing public health concern.[9,10]

The recent deaths of several high-profile athletes have resulted in significant public and scientific interest in the long-term effects of mTBI and chronic traumatic encephalopathy (CTE), a progressive neurodegenerative disease linked to repetitive brain trauma. Helmet sensor data indicate that football players can experience more than 1000 hits to the head over the course of a season.[11] This repetitive exposure has been associated with the development of CTE and changes in cognition, mood, and behavior that begin in the fourth to fifth decade of life and eventually progress to dementia.[12–17] Epidemiological studies indicate that professional football players are at least four times more likely to receive a diagnosis of memory impairment or dementia and have at least a three times greater risk of dying from a neurodegenerative disease, compared to the general population.[17,18] To date, all cases of neuropathologically confirmed CTE have had a history of repetitive brain trauma; therefore, repetitive brain trauma appears necessary for the development of the disease.[15,19] However, brain trauma alone is insufficient to lead to

[1]Boston University Alzheimer's Disease Center and [2]Center for the Study of Traumatic Encephalopathy, Boston University School of Medicine, Boston University, Boston, Massachusetts.
[3]Department of Psychology, University of Colorado at Colorado Springs, Colorado Springs, Colorado.
[4]Department of Biostatistics and [5]Data Coordinating Center, Boston University School of Public Health, Boston University, Boston, Massachusetts.
[6]Neurology Service, Veterans Affairs Boston Healthcare System, Jamaica Plain, Massachusetts.
Departments of [7]Neurology and [8]Pathology, Boston University School of Medicine, Boston, Massachusetts.
[9]Department of Neurosurgery, Emerson Hospital, Concord, Massachusetts.
[10]Department of Neurosurgery, Boston University School of Medicine, Boston University, Boston, Massachusetts.

neurodegeneration in all individuals (i.e., not everyone with repetitive TBI gets CTE).[15]

To date, relatively few studies have examined cognitive functioning in football players during life. Amen and colleagues found that active and retired football players scored in the bottom 50th percentile on three indices (attention/mental control, memory, and reasoning) of a computerized assessment of neuropsychological status.[20] Former university hockey and football players who sustained concussions have been found to perform worse on measures of memory and attention/executive function decades after their last concussion.[21] These studies indicate that executive functioning is impaired in former contact-sport athletes many years after the athlete's last exposure to brain trauma.

The long-term effects of repetitive brain trauma on cognition have yet to be examined using a standardized self-report measure of executive function. The Behavior Rating Inventory of Executive Function, adult version (BRIEF-A) was chosen for this study because of its use in clinical neuropsychological assessments and well-established normative data. Additionally, reports indicate that the BRIEF-A is sensitive to early executive deficits, before they might typically present on objective measures of cognitive function.[22] The aim of this study was to examine executive function in current and retired college and professional football players, a group at high risk of exposure to repetitive mTBI, using the BRIEF-A. We hypothesized that these football players would report more-frequent problems with executive functioning than healthy, same-age control participants. Because CTE symptoms typically present in the fourth or fifth decade of life, we hypothesized that football players over 40 years of age would report more-frequent problems than younger athletes.

Methods

This project was part of an ongoing longitudinal study examining cognitive function in current and former athletes. Inclusion criteria include being at least 18 years old and having a history of participation in organized sports at any level of competition. Recruitment methods include the following: (1) inclusion of the study on the Center's website and the website of the Sports Legacy Institute; (2) lectures and presentation at a variety of events for athletes at all levels of play; and (3) word of mouth. All participants are self-referred. This larger project (the Longitudinal Examination to Gather Evidence of Neurodegenerative Disease; LEGEND), requires completion of yearly telephone interviews and online questionnaires. Participants are sent an e-mail link to complete the online questionnaires, which include self-report measures of cognition, mood, and performance on activities of daily living. Demographic characteristics, athletic experience, and concussion history, as well as participant and family medical and psychiatric history, are also obtained. Subsequent to completion of the online questionnaires, participants are contacted by phone to complete the telephone interview. The present study included all college and professional football players in the LEGEND study at the time of data analysis.

Participants

Participants included 64 male current and retired football players, ranging from 25 to 81 years of age (mean, 47.0; standard deviation, 13.6). All LEGEND participants with a history of participation in college or professional football were selected for analysis. The football players were grouped by highest level achieved and age greater than or equal to 40. Demographic and athletic characteristics of the groups are listed in Table 1. All participants provided informed consent for the protocol approved by the Boston University Medical Center Institutional Review Board (Boston, MA).

Measures and procedures

Participants completed an online version of the BRIEF-A, a 75-item self-report measure of executive functioning in everyday activities over the past 30 days. Participants were instructed to answer the following question for each statement: ''During the past month, how often has each of the following behaviors been a problem?'' Responses use a three-point scale, scored as follows: never = 1; sometimes = 2; and often = 3. Higher scores indicate worse executive function. These responses yield an overall composite score (Global Executive Composite; GEC), two index scores [Behavioral Regulation Index (BRI) and Metacognition Index (MI)], and the following nine clinical scales: Inhibit; Shift; Emotional Control; Self-Monitor; Initiate; Working Memory; Plan/Organize; Task Monitor; and Organization of Materials. Each clinical scale includes 6–10 items. The BRI index is composed of the Inhibit, Shift, Emotional Control, and Self-Monitor

TABLE 1. DEMOGRAPHIC CHARACTERISTICS

Characteristic	*AP (n = 64)*	*CF (n = 35)*	*PF (n = 29)*	*< 40 (n = 22)*	*≥ 40 (n = 42)*
Mean age, years (SD)	47.0 (13.6)	45.9 (14.1)	48.3 (13.0)	33.0 (3.9)†	54.3 (10.8)
Age range	25–81	25–78	27–81	25–39	41–81
Education (terminal degree)					
High school/GED, %	1.6	0	3.4	0	2.4
Associates/certification, %	1.6	2.9	0	4.5	0
Bachelor's degree, %	65.6	57.1	75.9	68.2	64.3
Master's or doctoral degree, %	31.3	40	20.7	27.3	33.3
Athletic history					
Total years of football (SD)	13.0 (5.1)	9.5 (2.7)	17.2 (3.9)*	11.8 (4.3)	13.6 (5.4)
Years played in college (SD)	3.7 (1.0)	3.3 (1.3)	4.2 (.51)*	3.7 (1.1)	3.9 (0.85)
Years played professionally (SD)	3.0 (4.1)	N/A	6.4 (3.6)	2.2 (3.8)	3.6 (4.2)
Professional: college	N/A	N/A	N/A	8:14	21:21
Number of concussions (SD)	350.8 (2516.0)	24.9 (23.8)	758.1 (3771.7)	22.8 (223.2)	526.7 (3117.8)

< 40 indicates players 39 years of age and younger, whereas ≥ 40 indicates players 40 or more years of age.
*Significant differences between CF and PF (alpha = 0.05).
†Significant differences between < 40 and ≥ 40 ($p < 0.05$).
AP, all players; CF, college players; PF, professional players; SD, standard deviation; GED, General Educational Development.

subscales, and the MI index is composed of the Initiate, Working Memory, Plan/Organize, Task Monitor, and Organization of Materials subscales.

Concussion history was obtained during a phone interview. Participants were provided the following definition of concussion:

> "Some people have the misconception that concussions only happen when you black out after a hit to the head or when the symptoms last for a while. But, in reality, a concussion has occurred anytime you have had a blow to the head that caused you to have symptoms for any amount of time. These include: blurred or double vision, seeing stars, sensitivity to light or noise, headache, dizziness or balance problems, nausea, vomiting, trouble sleeping, fatigue, confusion, difficulty remembering, difficulty concentrating, or loss of consciousness. Whenever anyone gets a ding or their bell rung, that too is a concussion"

Based on this definition, participants were asked to state approximately how many total concussions they have had during their life.

Statistical analysis

Scores on the BRIEF-A were converted to age-appropriate T scores based on published normative data, which include 1050 participants selected to proportionally represent the U.S. population in regard to sex, race/ethnicity, education, and geographic region.[23] Elite football players may differ from this normative population in several ways, including exposure to repetitive brain trauma, physical stature (height and weight), educational attainment (generally higher), health (alcohol use, heart disease, arthritis, chronic pain, orthopedic issues, number of surgeries, depression, dementia, and use of medications), and health-related behaviors (increased alcohol use, decreased smoking, and illicit drug use).[24] For comparison of mean scores with normative data, one-sample *t*-tests were performed. For between-group comparisons, *t*-tests for two independent samples were performed. When indicated by Levene's test for equality of variances, degrees of freedom were adjusted to account for unequal variances. Because there were cases with zero counts in some cells, rates of clinically elevated scores (i.e., percent of individuals with a T score ≥ 65) were compared to additional normative data using Fisher's exact test. For the overall composite score (GEC) and index scores (BRI and MI), an alpha level of 0.05 was adopted. To control for type I errors, analyses of the nine clinical scales were conservatively adjusted for multiple comparisons using Bonferroni's correction (0.05/9 = 0.006). Analyses of the individual clinical scales were performed when significant group effects were observed on the overall composite score or one of the two index scores.

Results

Comparison between college and professional football players

Effects of competition level (i.e., professional vs. college) on the overall composite score and the two index scores were examined by independent sample *t*-tests. Scores on the GEC were similar between groups ($t(44.2) = 2.0$; $p = 0.06$). Professional and college football players indicated similar functioning on the BRI index ($t(49.3) = 1.9$; $p = 0.06$), but the professional athletes reported more-frequent executive functioning problems on the MI index ($t(42.7) = 2.4$; $p < 0.05$). Analyses of clinical scales revealed similar ratings between groups at each of the nine scales (all *p* values > 0.006). Given the similarity between groups, data from college and professional football players were combined for subsequent analyses.

Comparison between football players and normative data for healthy adults

Effects of participation in football were examined by one-sample *t*-tests comparing age-adjusted T scores with the known population mean of 50. Significant group differences were observed on GEC ($t(63) = 5.4$; $p < 0.05$), MI ($t(63) = 5.3$; $p < 0.05$), and BRI ($t(63) = 5.2$; $p < 0.05$). Analyses of the clinical scales indicated significant group effects on seven of the nine scales: Inhibit ($t(63) = 5.8$; $p < 0.006$); Shift ($t(63) = 4.4$; $p < 0.006$); Emotional Control ($t(63) = 4.9$; $p < 0.006$); Initiate ($t(63) = 4.6$; $p < 0.006$); Working Memory ($t(63) = 6.6$; $p < 0.006$); Plan/Organize ($t(63) = 3.9$; $p < 0.006$); and Task Monitor ($t(63) = 4.8$; $p < 0.006$). Differences between groups on Organization of Materials reached the corrected alpha level of 0.006, but was not below this threshold ($t(63) = 2.8$; $p = 0.006$), and groups were similar on Self-Monitor ($t(63) = 1.4$; $p = 0.16$). Across all scales, the football players indicated worse functioning than the normative sample.

Rates of clinically elevated scores (i.e., T scores ≥ 65) between groups were examined by Fisher's exact test. Significant group differences emerged on GEC ($x^2(1, n = 90) = 9.1$; $p < 0.05$), MI ($x^2(1, n = 90) = 13.3$; $p < 0.05$), and BRI ($x^2(1, n = 90) = 8.5$; $p = 0.05$). Analyses of the clinical scales indicated significant group effects on five of the nine scales: Inhibit ($x^2(1, n = 90) = 8.5$; $p < 0.006$); Shift ($x^2(1, n = 90) = 7.9$; $p < 0.006$); Initiate ($x^2(1, n = 90) = 9.1$; $p < 0.006$); Working Memory ($x^2(1, n = 90) = 13.3$; $p < 0.006$); and Plan/Organize ($x^2(1, n = 90) = 11.1$, $p < 0.006$). The rate of clinically elevated scores was similar between groups on the remaining four scales: Emotional Control ($x^2(1, n = 90) = 5.9$; $p = 0.02$); Self-Monitor ($x^2(1, n = 90) = 5.6$; $p = 0.02$); Task Monitor ($x^2(1, \text{n} = 90) = 4.5$; $p = 0.05$); and Organization of Materials ($x^2(1, n = 90) = 2.0$; $p = 0.27$). Across all scales, the football players had higher rates of clinically elevated scores than the normative sample.

Comparison between younger and older football players

Effects of age group (i.e., < 40 vs. ≥ 40 years) on the overall composite score and the two index scores were examined by independent sample *t*-tests. Older athletes indicated more-frequent problems overall ($t(62) = 2.7$; $p < 0.05$), on the BRI ($t(56.0) = 3.3$; $p = 0.05$); and on the MI indices ($t(62) = 2.1$; $p < 0.05$), when compared to younger athletes. Analyses of clinical scales revealed group differences on two of the nine scales. Older football players indicated experiencing more problems on the Emotional Control ($t(62) = 2.9$; $p < 0.006$) and Initiate ($t(55.8) = 3.2$; $p < 0.006$) clinical scales. Scores on the remaining scales were similar between groups, including Inhibit ($t(57.7) = 1.8$; $p = 0.08$), Shift ($t(62) = 2.5$; $p = 0.01$), Self-Monitor ($t(62) = 2.7$; $p = 0.01$), Working Memory ($t(62) = 1.4$; $p = 0.16$), Plan/Organize ($t(62) = 1.9$; $p = 0.07$), Task Monitor ($t(62) = 2.5$; $p = 0.02$), and Organization of Materials ($t(62) = 1.5$; $p = 0.14$; see Table 3).

Correlations between BRIEF-A and athletic history

Correlations between BRIEF-A scores, self-reported concussions, and years playing football were determined by Pearson's correlation coefficients for all participants, separately for level of play and age groups. The number of self-reported concussions was log-transformed because of the non-normal distribution of these data. Overall, 56 of the 64 participants (87.5%) reported experiencing 55 or fewer concussions. For the remaining 8 participants, 6 reported experiencing between 100 and 140 concussions, 1

Table 2. Comparison of Age-Adjusted T Scores between Football Players (College and Higher) and Normative Data for Healthy Adults on the BRIEF-A

	Football players[a]		*Football*[a] *vs. healthy adults*[b]		
	Mean (SD)	*Percent of T scores ≥65*	*T-score* p *value*	*Cohen's d*	*T scores ≥65* p *value*
Index scores					
BRI	58.2 (12.8)	26.6	0.000*	0.81	0.004*
MI	59.4 (14.2)	37.5	0.000*	0.91	0.000*
GEC	58.9 (13.2)	28.1	0.000*	0.87	0.002*
Clinical scales					
Inhibit	58.4 (11.5)	26.6	0.000*	0.85	0.004*
Shift	56.3 (11.4)	25.0	0.000*	0.63	0.005*
Emotional Control	58.0 (13.0)	26.6	0.000*	0.79	0.015
Self-Monitor	52.3 (13.0)	18.8	0.159	0.23	0.018
Initiate	58.1 (14.1)	28.1	0.000*	0.79	0.002*
Working Memory	62.4 (15.0)	37.5	0.000*	1.20	0.000*
Plan/Organize	56.9 (14.1)	32.8	0.000*	0.67	0.001*
Task Monitor	57.6 (12.6)	28.1	0.000*	0.75	0.035
Organization of Material	54.3 (11.9)	14.1	0.006	0.43	0.162

Scores from football players were compared to age-adjusted normative data published in the BRIEF-A manual.
[a]$n = 64$.
[b]$n = 1050$.
*Significant group differences (index scores, alpha < 0.05; clinical scales, alpha < 0.006).
BRI, Behavioral Regulation Index; MI, Metacognition Index; GEC, Global Executive Composite; SD, standard deviation.

reported experiencing approximately 350 concussions, and 1 reported experiencing approximately 20,000 concussions. These analyses were performed to determine if total years of play and/or number of concussions contributed to the between-group findings. In the overall sample, total number of years played correlated with Working Memory ($r = 0.29$; $p < 0.05$), and number of self-reported concussions correlated with Emotional Control ($r = 0.26$; $p < 0.05$) and Initiate ($r = 0.32$; $p < 0.05$). In the younger than 40 group, number of self-reported concussions correlated with Inhibit ($r = 0.54$; $p < 0.05$). In the older than 40 group, total number of years played correlated with Working Memory ($r = 0.37$; $p < 0.05$). No other correlations were significant.

Table 3. Comparison Between Age-Adjusted T Scores on BRIEF-A between Players Younger and Older Than 40 Years

	Football players less than 40 years of age (n = 22)	*Football players 40 and older* (n = 42)	p *value*
Index scores[a]			
BRI*	52.0 (9.4)	61.5 (13.2)	0.002
MI*	54.5 (13.9)	62.0 (13.8)	0.043
GEC*	53.1 (10.7)	62.0 (13.5)	0.010
Clinical scales[b]			
Inhibit	55.3 (8.5)	60.1 (12.5)	0.075
Shift	51.5 (9.9)	58.8 (11.4)	0.014
Emotional Control*	51.9 (9.9)	61.2 (13.4)	0.005
Self-Monitor	46.5 (10.1)	55.4 (13.4)	0.008
Initiate*	51.4 (10.5)	61.6 (14.6)	0.002
Working Memory	58.7 (12.0)	64.3 (16.2)	0.158
Plan/Organize	52.4 (11.8)	59.2 (14.7)	0.067
Task Monitor	52.4 (10.9)	60.4 (12.7)	0.015
Organization of Material	51.2 (10.3)	55.9 (12.5)	0.138

All means and standard deviations are reported.
[a]Alpha level = 0.05.
[b]Alpha level was adjusted to 0.006.
*Statistically significant.
BRI, Behavioral Regulation Index; MI, Metacognition Index; GEC, Global Executive Composite.

Discussion

In this study, we examined a self-report measure of executive function in current and retired college and professional football players, a group with high exposure to repetitive brain trauma. Overall, we found that football players reported more-frequent problems with executive function in everyday activities, when compared to published normative data for healthy individuals of the same age and representative of the U.S. population in regard to sex, race/ethnicity, education, and geographic region. Scores were elevated overall, as well as on specific indices of the ability to control behavior and emotional responses and the ability to methodically solve problems through planning, organization, and sustaining effort. Despite higher scores overall, considerable variability was observed across participants, indicating that not all elite football players experience executive dysfunction.

It should be highlighted that the football players reported a normal frequency of problems on monitoring the effects of their behavior on others. Taken together, this profile suggests that football players may be aware of any effects they may have on others, but are unable to change their behavior because of weaknesses in thinking flexibly and inhibition. It is plausible that this may contribute to depression observed in former athletes with CTE.[15] It should be emphasized that executive dysfunction has several etiologies, and not all football players with these symptoms will develop CTE.

Consistent with our hypothesis, football players 40 years of age and older reported more frequent problems with the ability to control behavior and emotional responses, even after the data were corrected for age. This finding provides additional evidence to suggest that problems with executive function in football players develop or worsen after 40 years of age. Alternatively, differences between age groups could be a cohort effect, reflecting changes in professional

football over the decades (e.g., development of new protective equipment or differences in individuals that choose to participate). Longitudinal studies are needed to better understand this finding.

Although we believe this study has several strengths, there are also a number of important limitations that require discussion. Scores on the BRIEF-A were compared to normative data, which is not an ideal comparison group for elite athletes. Future studies would benefit from having a comparison group of elite non-contact-sport athletes. If results were similar, the findings would further suggest that this executive dysfunction results from repeated mTBI. Because of recent publicity surrounding CTE and the self-referral in our study, it may be that only symptomatic individuals who were concerned about their cognitive functioning volunteered. If this were the case, however, we would have expected to observe very few scores in the normal range. In contrast, nearly one third (31.3%) of the participants had overall scores at or below the expected value for their age (i.e., T score of 50), and for the majority of participants (71.8%), the overall score was below the clinically meaningful threshold (i.e., T score of 65). Because of the inclusion of current and recently retired players, it is possible that some of the executive function problems reported stem from residual postconcussive syndrome. In this case, we would have expected to find higher scores in the younger players. In contrast, we observed higher scores in football players older than 40. Given the retrospective nature of this study, it is impossible to determine whether these findings stem from the effects of participation in football or whether individuals with these characteristics seek out this sport initially. Future prospective studies examining change in executive function over time are needed. Although the BRIEF-A has good convergent validity with other questionnaires, future studies will benefit from also using objective measures of executive functioning in addition to self-report measures. Finally, we did not exclude individuals with a history of repeated brain trauma from participation in other contact sports or non-sport-related TBIs, which may have also affected the results.

In summary, our results indicate that college and professional football players experience more problems with executive functions in everyday activities than would be expected for their age, and these symptoms appear to develop or worsen in the fifth decade of life. Future longitudinal studies are needed to confirm these initial results. The findings are in accord with a growing body of evidence that participation in football may be associated with the development of cognitive changes and dementia observed in individuals with CTE.

Acknowledgments

This work was supported by the Boston University Alzheimer's Disease Center (NIA P30 AG13846, supplement 0572063345-5), the National Institutes of Health (R01NS078337), a grant from the National Operating Committee on Standards for Athletic Equipment, the Sports Legacy Institute, the Center for the Integration of Medicine and Innovative Technology, and an unrestricted gift from the National Football League. A portion of this research was presented at the 2012 Military Health System Research Symposium, in Fort Lauderdale, FL, August 13–16, 2012.

The authors thank all the individuals who participated in this study. Brian Stamm and Andrew Brennan provided expert technical support.

Author Disclosure Statement

No competing financial interests exist.

References

1. Faul, M Z.L., Wald, M.M., and Coronado, V.G. (2010). Traumatic brain injury in the United States: emergency department visits, hospitalizations, and deaths. Centers for Disease Control and Prevention, National Center for Injury Prevention and Control: Atlanta, GA.
2. Control C.f.I.P.a. (2003). Report to Congress on mild traumatic brain injury in the United States: steps to prevent a serous public health problem. Centers for Disease Control and Prevention: Atlanta, GA.
3. Finkelstein, E., Corso, P., and Miller, T. (2006). *The Incidence and Economic Burden of Injuries in the United States*. Oxford University Press: New York.
4. Dikmen, S.S., Corrigan, J.D., Levin, H.S., Machamer, J., Stiers, W., and Weisskopf, M.G. (2009). Cognitive outcome following traumatic brain injury. J. Head Trauma Rehabil. 24, 430–438.
5. Langlois, J.A., Rutland-Brown, W., and Wald, M.M. (2006). The epidemiology and impact of traumatic brain injury: a brief overview. J. Head Trauma Rehabil. 21, 375–378.
6. Daneshvar, D.H., Nowinski, C.J., McKee, A.C., and Cantu, R.C. (2011). The epidemiology of sport-related concussion. Clin Sports Med. 30, 1–17, vii.
7. Hootman, J.M., Dick, R., and Agel, J. (2007). Epidemiology of collegiate injuries for 15 sports: summary and recommendations for injury prevention initiatives. J. Athl. Train. 42,311–9.
8. Gessel, L.M., Fields, S.K., Collins, C.L., Dick, R.W., and Comstock, R.D. (2007). Concussions among United States high school and collegiate athletes. J. Athl. Train. 42, 495–503.
9. Promotion N.C.f.C.D.P.H. (2006). Behavioral risk factor surveillance system: exercise: Centers for Disease Control and Prevention: Atlanta, GA.
10. National Council of Youth Sports. (2008) Report on Trends and Participation in Organized Youth Sports. National Council of Youth Sports: Stuart, FL.
11. Gysland, S.M., Mihalik, J.P., Register-Mihalik, J.K., Trulock, S.C., Shields, E.W., and Guskiewicz, K.M. (2012). The relationship between subconcussive impacts and concussion history on clinical measures of neurologic function in collegiate football players. Ann. Biomed. Eng. 40, 14–22.
12. Omalu, B.I., DeKosky, S.T., Hamilton, R.L., Minster, R.L., Kamboh, M.I., Shakir, A.M., and Wecht C.H. (2006). Chronic traumatic encephalopathy in a national football league player: part II. Neurosurgery 59, 1086–1092; discussion, 1092–1093.
13. Omalu, B.I., DeKosky, S.T., Minster, R.L., Kamboh, M.I., Hamilton, R.L., and Wecht, C.H. (2005). Chronic traumatic encephalopathy in a National Football League player. Neurosurgery 57, 128–134; discussion, 134.
14. Omalu, B.I., Hamilton, R.L., Kamboh, M.I., DeKosky, S.T., and Bailes, J. (2010). Chronic traumatic encephalopathy (CTE) in a National Football League Player: case report and emerging medicolegal practice questions. J. Forensic Nurs. 6, 40–46.
15. McKee, A.C., Cantu, R.C., Nowinski, C.J., Hedley-Whyte, E.T., Gavett, B.E., Budson, A.E., Santini, V.E., Lee, H.S., Kubilus, C.A., and Stern, R.A. (2009). Chronic traumatic encephalopathy in athletes: progressive tauopathy after repetitive head injury. J. Neuropathol. Exp. Neurol. 68, 709–735.
16. McKee, A.C., Gavett, B.E., Stern, R.A., Nowinski, C.J., Cantu, R.C., Kowall, N.W., Perl, D.P., Hedley-Whyte, E.T., Price, B., Sullivan, C., Morin, P., Lee, H.S., Kubilus, C.A., Daneshvar, D.H., Wulff, M., and Budson, A.E. (2010). TDP-43 proteinopathy and motor neuron disease in chronic traumatic encephalopathy. J. Neuropathol. Exp. Neurol. 69, 918–929.
17. Guskiewicz, K.M., Marshall, S.W., Bailes, J., McCrea, M., Cantu, R.C., Randolph, C., and Jordan, B.D. (2005). Association between recurrent concussion and late-life cognitive impairment in retired professional football players. Neurosurgery 57, 719–726; discussion, 726.
18. Lehman, E.J., Hein, M.J., Baron, S.L., and Gersic, C.M. (2012). Neurodegenerative causes of death among retired National Football League players. Neurology 12, 1970–1974.
19. McKee, A.C., Stern, R.A., Nowinski, C.J., Stein, T.D., Alvarez, V.E., Daneshvar, D.H., Lee, H.S., Wojtowicz, S.M., Hall, G., Baugh, C.M., Riley, D.O., Kubilus, C.A., Cormier, K.A., Jacobs, M.A., Martin, B.R., Abraham, C.R., Ikezu, T., Reichard, R.R., Wolozin, B.L.,

Budson, A.E., Goldstein, L.E., Kowall, N.W., and Cantu, R.C. (2013). The spectrum of disease in chronic traumatic encephalopathy. Brain Jan 29. doi: 10.1093/brain/aws307.

20. Amen, D.G., Newberg, A., Thatcher, R., Jin, Y., Wu, J., Keator, D., and Willeumier, K. (2011). Impact of playing American professional football on long-term brain function. J. Neuropsychiatry Clin. Neurosci. 23, 98–106.
21. De Beaumont, L., Theoret, H., Mongeon, D., Messier, J., Leclerc, S., Tremblay, S., Ellemberg, D., and Lassonde, M. (2009). Brain function decline in healthy retired athletes who sustained their last sports concussion in early adulthood. Brain 132, 695–708.
22. Rabin, L.A., Roth, R.M., Isquith, P.K., Wishart, H.A., Nutter-Upham, K.E., Pare, N., Flashman, L.A., and Saykin, A.J. (2006). Self- and informant reports of executive function on the BRIEF-A in MCI and older adults with cognitive complaints. Arch. Clin. Neuropsychol. 21, 721–732.
23. Roth, R.M., Isquith, P.K., and Gioia, G.A. (2005). *BRIEF-A: Behavior Rating Inventory of Executive Function—Adult Version: Professional Manual*. Psychological Assessment Resources: Lutz, FL.
24. Weir, D.R., Jackson, J.S., and Sonnega, A. (2009). National football league player care foundation. Study of retired NFL players. Institute for Social Research, University of Michigan, 1–37.

Address correspondence to:
Robert A. Stern, PhD
Center for the Study of Traumatic Encephalopathy
Boston University
72 East Concord Street, Suite B7800
Boston, MA 02118

E-mail: bobstern@bu.edu

EXHIBIT 78

REGRESSING (/)

(/)

REGRESSING

(/)

(/)

Search

Can Science See Inside An NFL Player's Skull Before It's Too Late? (http://regressing.deadspin.com/5920006/can-science-see-inside-an-nfl-players-skull-before-its-too-late)

(http://kylenw.kinja.com)

Kyle Wagner (http://kylenw.kinja.com)

Filed to: BAD BRAINS (/TAG/BAD-BRAINS) 6/21/12 9:00am (http://regressing.deadspin.com/5920006/can-science-see-inside-an-nfl-players-skull-b

66,140 2

EXPAND

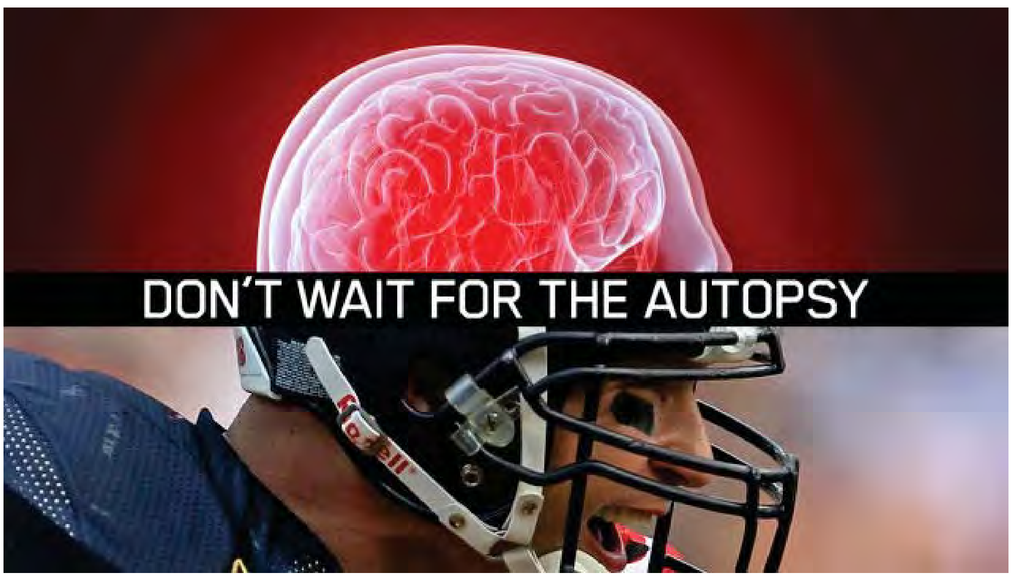

Chronic traumatic encephalopathy, or CTE, is a diagnosis for dead people. Last month, Junior Seau was found in his home in Oceanside, Calif., with a fatal self-inflicted gunshot wound to the chest. A familiar sequence unfolded: His brain was requested by both the Brain Injury Research Institute and Boston University's Center for the Study of Traumatic Encephalopathy—the two main brain banks chasing damage in former football players. If the family consents, the brain will be sliced open and put under a microscope.

Given Seau's profession and the nature of his demise, the expectation is that the tissues will show a buildup of a protein called tau, creating tangles like the ones found in victims of Alzheimer's disease. But so what? It's one more brain, to go with the 60-plus brains of former players who have already demonstrated postmortem signs of CTE.

The question, after a decade of brain-slicing autopsies, is when any of this will help players before they're dead. Doctors can't just crack open living patients' skulls and lop off slices of their brains to stick under a microscope.

But new research at UCLA is using a cutting-edge biomarker that can attach itself to tau protein tangles so that they show up on PET scans of living subjects. Dr. Gary Small is currently running a pilot study on retired NFL players, imaging their brains in place. If he is successful, his work would reorient the science of head injuries around saving lives instead of merely contextualizing deaths.

"I've always sort of thought of tau imaging as the holy grail on the issue of chronic brain damage, especially CTE," said Dr. Julian Bailes, one of the founders of the Brain Injury Research Institute (BIRI).

The grail isn't in hand yet. But the marker that attaches to tau is among the most promising of an assortment of research projects seeking to make CTE something other than an after-the-fact conclusion. Tools to see CTE in living players, tests and techniques honed on other forms of brain damage that may be able to track the disease's progress—science is trying to get inside the skull, before it's too late.

At The Frontier Of Head-Injury Science

In 2009, the NFL, under heavy fire from the House Judiciary Committee, acknowledged for the first time the long-term consequences of concussions. Since then, the league's ideas about how to protect the living have focused on improving the equipment (better helmets and thighpads) and conspicuously fining defensive players for especially gruesome-looking hits. Non-NFL-affiliated studies have tended to coalesce around those issues. We've measured the force of collisions in mouthguards and pads, and we know the effect of those anti-concussion helmets, too.

But taken as a whole, the efforts to quell or at least understand CTE have been, to this point, a mix of the cynical, the haphazard, and the fatalistic. There is real value in gathering data about the force of impacts, but the context has often been backward-looking, substantiating science that's no longer really in question. The brain donation and autopsy, for instance, is now more of a mourning rite than a marshalling of fresh evidence.

The NFL has been too busy cosseting itself against any potential legal liability and seeking out second opinions to ask the only question left: What now? The frontiers of CTE research—living patient diagnosis, prevention, risk assessment, *cures*—have been largely left unexplored.

(The NFL did announce a promising study (http://www.nytimes.com/2011/10/04/sports/football/nfl-plans-more-scientific-study-of-concussions.html) late last year, but there have been few details since about when and how it might launch. And it's now been essentially outflanked by a new joint study (http://espn.go.com/blog/ncfnation/post/_/id/62166/b1g-ivy-doing-vital-work-on-concussions) between the Big Ten and the Ivy League that will get underway this year.)

It's not as if the league hasn't had time to do real homework. It's been 10 years since Dr. Bennet Omalu first cut into Mike Webster's brain and discovered CTE, and seven years since Omalu's work appeared in the July 2005 issue of *Neuroscience*, where it was shouted down by the NFL.

Dozens of dead men's brains later, the disbelievers have mostly come around. At its core, CTE is a neurodegenerative brain disease, not much different from Alzheimer's, Parkinson's, or early-onset dementia. It breaks part of your brain, and that affects how you behave and function. But unlike other cases of cognitive decline, we believe we know the root cause: repeated blunt head trauma.

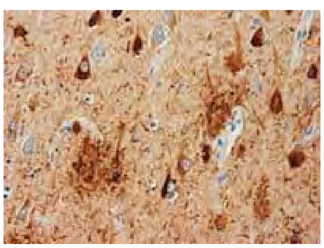
The research could have a profound effect on the NFL and possibly the NCAA. Being able to track the buildup of tau (pictured) is the key to any future serious player safety regime.

While we don't have a cure for CTE's closest analogs, having that starting point makes a big difference. If we can see how the disease unfolds, we have a chance of stopping it. Thus: Gary Small's UCLA research into scanning living subjects. It's funded by BIRI, which was founded by Omalu, Bailes, and Robert Fitzsimmons.

At the center of the study is a patented radioactive biomarker that Small co-invented for diagnosing Alzheimer's disease. The marker attaches itself to both tau protein tangles and amyloid plaques, the two elements necessary to diagnose Alzheimer's. There are other markers that attach to plaques, but this specific marker, $[^{18}F]$FDDNP, is the only one known to lock onto tau. In the absolute simplest terms, this is the only known substance in the world that can make CTE show up on a scan in living patients.

PET imaging tech is half a century old, and though FDDNP is relatively new, it's still been around for years. So it's strange to think about the marker being on the cutting edge of a fairly recently discovered brain disease. If the marker can find and pinpoint CTE, why hadn't anyone tried it before now? And for that matter, why isn't it already in use?

More than finding answers, science is about asking the right questions. For something like FDDNP to be tested on NFL players, the thought not only has to occur to someone, but that someone then has to get together some grants or other funding, and some applicable test subjects.

The case of something like PET imaging is doubly difficult, because a PET scan is literally a matter of injecting a radioactive material into your patients and using a giant Geiger counter to see where it lands. Radiation exposure is tracked closely, and a person can receive only a limited number of scans per year, Small said, though he adds that "the only potential side effects people get from scans is a bruise where the IV goes in, or a backache from lying in the scanner."

Small, whose background is in geriatric psychology and Alzheimer's disease, came to CTE research when the chancellor of West Virginia University introduced him to Bailes, who was at WVU at the time. Small's initial study has been funded by BIRI, and Bailes helped refer retired players to Small to try out the scan.

The study is still a pilot program, and there's work to be done before it can be translated into something we can use to diagnose developing cases of CTE—mainly stemming from the fact that FDDNP locks onto not just tau, but the amyloid plaques as well. Still, a biomarker would be perhaps the most important development in the field since Omalu looked at a slide of Webster's brain and saw tau's telltale brown and red splotches (http://www.gq.com/sports/profiles/200909/nfl-players-brain-dementia-study-memory-concussions). Small couldn't share the specific results of his studies because they haven't been published yet, but he was confident. "We think this is going to be a very helpful way to better understand and identify people who are at risk," he said.

"We've autopsied more players than anyone—more than 30 now—and while the science is intriguing, we can only make the diagnosis after death," Bailes said. Small's work, he added, "gives us hope we'll be able to diagnose and identify risk in living patients."

If the scans are effective, they could have a profound effect on the NFL and possibly the NCAA. Being able to track the buildup of tau is the key to any future serious player safety regime. This would likely require regular PET scans—yearly, maybe, or twice a season. An extreme case of CTE—like Webster's—would have a better chance of being caught, especially in the latter stages of a player's career, when his protein levels would be higher.

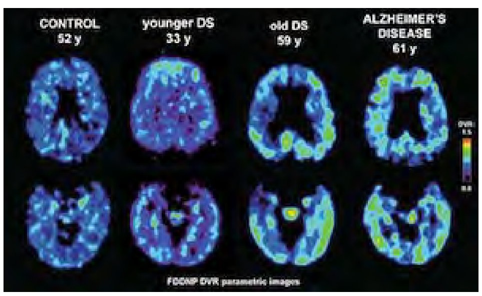

PET scan, similar to Small's work with CTE, of brain amyloid and tau in adults with Down syndrome.

But even with reliable scans, the risk factors and the rate of tau accumulation would differ from player to player. So Small's group has been looking at ways to refine the risk assessment available to players. "We're looking at genetic factors, a player's position, other behaviors that worsen brain health like smoking or drinking," he said. He's also keeping an eye out for other signs or markers that could be used to identify tau. If, for example, a specific change in a patient's blood were to occur when there's a buildup of tau, maybe a blood test could offer an affordable and less-invasive alternative to the PET scan.

Cheaper alternatives are a crucial point, too. Right now, each scan costs about $5,000. The price could drop as more companies and groups license FDDNP from UCLA for research. But the scans still probably won't get into the range where the average high school or Division III college could afford to have their players tested multiple times a year.

Knowing When To Stop

In Las Vegas, Dr. Charles Bernick is attacking the same problem from a different angle. Instead of looking for CTE itself, Bernick wants to know how the disease spreads and changes its victim over time. He's wrapping up the first year of an ongoing study tracking the cognitive health of over 100 boxers and MMA fighters, some of whom enlisted at the urging of a family member or spouse who'd started to notice changes in behavior. The goal of the study is to pinpoint when, exactly, a fighter should hang up the gloves.

The Professional Fighters Brain Health Study at the Cleveland Clinic's Lou Ruvo Center for Brain Health pulls from the center's experience with similar diseases, like Parkinson's, to develop a working *modus operandi* for attacking CTE as a traditional brain disease. (The difference, of course, is that those other diseases are a constant deterioration of brain function, while CTE is caused by intermittent brain trauma.) The study uses a combination of MRI scans and computerized cognitive tests—exercises ranging from simple memory tests to questions about what the

fighters did or felt on certain occasions—to track how the subjects' brains and cognitive abilities change or degrade as their careers advance. If it can map the trajectory of CTE, we can not only extrapolate how much is too much, but use that information to begin working on cures or preventative measures—not just for boxing and MMA, but for all sports and occupations that pose a risk of CTE.

Bernick hasn't been in contact with the NFL. "It wouldn't be a bad idea in the field for all the oars to be rowing in the same direction," he said. "So if the NFL and hockey and the military were collecting core information, we'd learn a lot faster."

So far, Bernick's team has mapped out a regimen to test fighters at regular intervals for any signs of cognitive decline. The process, which involves computer-based cognitive tests, speech analysis, and thorough MRI scans, closely resembles the tests administered to Alzheimer's and EOD patients.

The MRI in particular is noteworthy. Like PET scans, it's an old technology that can be augmented by asking new and better questions. Specifically, Bernick is trying to hunt down CTE by measuring, comparatively, the size of certain parts of the brain over time, looking for swelling or scar tissue; comparing the brain's conductivity in a resting state to when it's active; and examining blood-vessel buildup, which happens around tau protein.

It's not as easy as just tossing a marker into the brain and firing up a PET scan, but it could be far more scalable outside of the lab.

There are some compromises, though, in the interest of making the test less time-consuming for fighters and other athletes. Unlike Alzheimer's diagnostics, for example, family and friends aren't brought in for cross-referencing on the cognitive tests, and there isn't a genetic analysis of close and distant relatives.

"There's way more that we need to do," Bernick said, "But we had to make it practical. The whole testing takes about two hours to do. It has to be tools you can use anywhere, and it's probably not realistic to expect everyone to go in for a two-hour neuropsych test, but maybe a 20-minute computerized test will do."

The preliminary findings have been suggestive. The fighters were split into three groups: those who had fought for fewer than six years, those who had fought for between six and 12 years, and those who had fought for more than 12 years. They showed a marked decline in cognitive ability from group to group. At six years, there was some drop-off; at 12 years, there was a much larger drop-off.

The six-year groupings were arbitrary, and the data will be shuffled some to try and get a more accurate line of demarcation. Year 2 also introduces retired fighters to the study, so new controls for age will have to be enacted, and more frequent check-ins would obviously be ideal. But for now, it's a starting point. Year over year, the data could be used to pick out different influences: genetic traits that might make humans resistant to CTE, various fighting styles, safe and dangerous layoff periods between fights.

And, of course, there will be post-mortem data. The clinic has made arrangements to supply many of the fighters' brains to one of the large brain banks involved in CTE research.

The important thing to remember about this research—all medical research, really—is that it's not looking to nail down a universal imperative. The surgeon general doesn't tell you the maximum number of cigarettes you're allowed to smoke, or the maximum poundage of cheeseburgers you should eat. So there will not be, say, a scientifically validated eight-year limit on fighting or contact sports. Instead, Bernick is hoping to build a tool for evaluating whether individual fighters should be allowed to continue fighting.

"If you're 38 years old and go to the [Nevada Athletic Commission] to be relicensed, what do they have to go on?" he said. "Maybe the last few fights' performance. But if there was information available to them, they would use it."

Bernick said his group has considered using information from the UCLA PET scans but is holding off because the marker isn't specific to tau itself, and there's still a chance that a tau-only agent will be found.

For their part, the fighters say that they're going to take the results seriously. "If they know that they're sustaining damage to their brain, they would stop," Bernick said. "Maybe a 22-year-old wouldn't say that, but it kind of evolves as you mature. I'm not sure totally people would ignore it. There are regulatory agencies who should be looking at this too. Hypothetically, if you fought eight years, you're required now to get an MRI scan once a year, or a computerized cognitive scan twice a year. If it's more severe, maybe you'd have to stop."

Padding The Inside Of The Skull

Brain injuries in football happen because of a phenomenon that Bailes, now co-director of NorthShore Neurological Institute, calls "brain slosh." "That's where the brain is free to move around inside the skull, regardless of helmets or external protection, because it floats inside a bath of fluid called Cerebral Spinal Fluid (CSF)," he explained. "Despite the fact that sports and the military looks at brain protection from the outside, we think you have to look at it from the inside."

In fact, Bailes is working on an absurdly simple accessory that could protect brains from being injured in the first place.

A rendering of the "internal jugular vein compression device." Courtesy Neurosurgery.

Think of it this way: In a collision, the brain is basically driving without a seatbelt or an airbag. While better helmets and the banning of helmet-to-helmet detonations might help keep your skull intact, they would do nothing to stop the brain from smashing into the windshield in even minor collisions. So how do you stop the brain from taking a beating on every routine block, tackle, and other impact—the real killers?

Bailes's answer to this brain slosh amounts to stuffing the whole car full of packing peanuts. His newest research takes groups of rats and puts a small, circular device around their necks, compressing their internal jugular veins. That increases the volume of blood in the skull, which creates added pressure on the brain, locking it in place. In theory, that should keep the brain's movement inside the skull more in line with the skull's own movement, allowing all the new space-age helmets to do their jobs.

So far, Bailes's team has seen a 30 percent increase in cranial pressure, and, after concussing the rats and examining the resulting computer models, an 80 percent drop in the precursors to amyloid protein. "This was only a proof-of-concept pilot study, and it hasn't been proven in humans, but we think the theory is sound," he said. "If it moves forward, we're going to expand to a broader group of patients, and we hope to do that sooner rather than later."

If the research can be replicated and no unforeseen safety concerns pop up—neither of which is guaranteed in research like this—there are already people and players volunteering as test subjects. Why wouldn't there be? If a simple necklace could reduce the accumulation of brain injury, and there is virtually no downside to wearing it, isn't that worth whatever minor discomfort it causes and a few hours a year of testing?

Who Will Pay For The Future?

But for all the practical upside of these projects, it's hard to make ends meet. I asked Bernick where he hopes his project tracking fighters' brains will be in five or 10 years. He replied: "I mean, before anything else, we hope to still be here in five or 10 years. The major goal is to keep the thing going."

The fighter brain-health study costs about $250,000 a year, but that number's misleading, because so much of what goes into the study—tests, scans, and most crucially, man-hours—is donated by the Cleveland Clinic and its staff. "Without that much help, it would probably cost twice as much," Bernick said.

The NFL's latest collective bargaining agreement sets aside $100 million to put toward research, much of which is expected to go to brain injury. But so far, only $1 million has been distributed—to Boston University's CSTE. This issue of funding—in Las Vegas, in tau protein imaging, in all of the studies that haven't or won't get off the ground—is more difficult than it seems.

The Nevada Athletic Commission is deeply interested, and supportive, of the Cleveland study, as are big time fight promoters like Bob Arum's Top Rank and Oscar De La Hoya's Golden Boy. "Everybody at the gyms around here have been very great about this," Bernick said. But despite financial uncertainty, the study hasn't taken money from any of them. "An interesting dilemma is where you get your funding, and conflicts of

interest," he explained. "Doing studies like this requires funding, but if you're heavily indebted in an agency that has a vested interest, there can be a view of a conflict of interest." That's also why he hasn't reached into the NFL's $100 million pockets yet either, though he absolutely would if it came down to a decision to accept funding or discontinue the study.

For Small's research into the tau protein biomarker, it's partially a matter of getting the word out. Because FDDNP is owned by UCLA, it can be licensed to any pharmaceutical company that wants to use it for studies. (Siemens licensed the marker for non-CTE research for a few years, but ultimately abandoned it.) "That would help drive the cost down, especially for the scans, but we'd still need further grants," Small said. The group has applied for an NIH grant, and submitted several studies and ideas, but it hasn't found any additional funding. Would he consider turning to the NFL and its $100 million slush fund? "Absolutely," he said, "if there are no strings attached. I understand the financial pressure the NFL is facing, but I'd hope that they want what's best for the players."

What does it mean for the viability of brain-injury research if even tau biomarking—the holy grail—has trouble finding backers? The logical place to stage a project like that would be one of those huge, überprofitable biomedical conglomerates. That's not happening. For competitive reasons, the companies won't talk about business strategies and future plans on the record, but the implication is unmistakable: There is no money in it. Not yet, anyway.

As with the search for a tau protein biomarker, there just isn't the widespread need for continued research in CTE the way there is for other forms of brain deterioration. A representative at one company who asked to not be named explained that, while recent talk about pulling the military into the ongoing brain-injury discussion could go a long way toward making the financials work, it still wouldn't be enough. Despite all the attention it's gotten, a health crisis affecting wealthy young celebrities in America's most popular sport is still only a niche concern.

"It's not like cancer, where your constituency is everyone, or even Alzheimer's, where there are millions," he said. "We just don't get hit in the head very often."

Kyle Wagner is a writer for Gizmodo (http://Gizmodo.com). Top image by Jim Cooke.

EXHIBIT 79

Cell PRESS

Neuron
Article

Imaging of Tau Pathology in a Tauopathy Mouse Model and in Alzheimer Patients Compared to Normal Controls

Masahiro Maruyama,[1,10] Hitoshi Shimada,[1,10] Tetsuya Suhara,[1] Hitoshi Shinotoh,[1] Bin Ji,[1] Jun Maeda,[1] Ming-Rong Zhang,[1] John Q. Trojanowski,[2] Virginia M.-Y. Lee,[2] Maiko Ono,[1] Kazuto Masamoto,[1] Harumasa Takano,[1] Naruhiko Sahara,[3,5,6] Nobuhisa Iwata,[4] Nobuyuki Okamura,[7] Shozo Furumoto,[7] Yukitsuka Kudo,[8] Qing Chang,[9] Takaomi C. Saido,[4] Akihiko Takashima,[3] Jada Lewis,[5,6] Ming-Kuei Jang,[9] Ichio Aoki,[1] Hiroshi Ito,[1] and Makoto Higuchi[1,*]

[1]Molecular Imaging Center, National Institute of Radiological Sciences, 4-9-1 Anagawa, Inage-ku, Chiba, Chiba 263-8555, Japan
[2]Center for Neurodegenerative Disease Research, University of Pennsylvania Perelman School of Medicine, Third Floor HUP-Maloney, 36th and Spruce Streets, Philadelphia, PA 19104, USA
[3]Laboratory for Alzheimer's Disease
[4]Laboratory for Proteolytic Neuroscience
RIKEN Brain Science Institute, 2-1 Hirosawa, Wako, Saitama 351-0198, Japan
[5]Center for Translational Research in Neurodegenerative Disease
[6]Department of Neuroscience
University of Florida, 1275 Center Drive, Gainesville, FL 32610, USA
[7]Department of Pharmacology, Tohoku University Graduate School of Medicine, 2-1 Seiryo-machi, Aoba-ku, Sendai, Miyagi 980-8575, Japan
[8]Clinical Research, Innovation and Education Center, Tohoku University Hospital, 1-1 Seiryo-machi, Aoba-ku, Sendai, Miyagi 980-8574, Japan
[9]Institute for Applied Cancer Science, MD Anderson Cancer Center, 1901 East Road, Houston, TX 77054, USA
[10]These authors contributed equally to this work
*Correspondence: mhiguchi@nirs.go.jp
http://dx.doi.org/10.1016/j.neuron.2013.07.037

SUMMARY

Accumulation of intracellular tau fibrils has been the focus of research on the mechanisms of neurodegeneration in Alzheimer's disease (AD) and related tauopathies. Here, we have developed a class of tau ligands, phenyl/pyridinyl-butadienyl-benzothiazoles/benzothiazoliums (PBBs), for visualizing diverse tau inclusions in brains of living patients with AD or non-AD tauopathies and animal models of these disorders. In vivo optical and positron emission tomographic (PET) imaging of a transgenic mouse model demonstrated sensitive detection of tau inclusions by PBBs. A pyridinated PBB, [^{11}C]PBB3, was next applied in a clinical PET study, and its robust signal in the AD hippocampus wherein tau pathology is enriched contrasted strikingly with that of a senile plaque radioligand, [^{11}C]Pittsburgh Compound-B ([^{11}C]PIB). [^{11}C]PBB3-PET data were also consistent with the spreading of tau pathology with AD progression. Furthermore, increased [^{11}C]PBB3 signals were found in a corticobasal syndrome patient negative for [^{11}C]PIB-PET.

INTRODUCTION

Hallmark pathologies of Alzheimer's disease (AD) are extracellular senile plaques consisting of aggregated amyloid β peptide (Aβ) and intraneuronal neurofibrillary tangles (NFTs) composed of pathological tau fibrils, while similar tau lesions in neurons and glia are also characteristic of other neurodegenerative disorders, such as progressive supranuclear palsy (PSP) and corticobasal degeneration (CBD), that are collectively referred to as tauopathies (Ballatore et al., 2007). The discovery of *tau* gene mutations in a familial form of tauopathy, known as frontotemporal dementia and parkinsonism linked to chromosome 17 (FTDP-17), and subsequent studies of transgenic (Tg) mice expressing human tau with or without these mutations, clearly implicate pathological tau in mechanisms of neurodegeneration in AD and related tauopathies (Ballatore et al., 2007). Thus, there is an urgent need for tau imaging techniques to complement Aβ amyloid imaging methods that now are widely used.

In vivo imaging modalities, as exemplified by positron emission tomography (PET) (Klunk et al., 2004; Small et al., 2006; Kudo et al., 2007; Maeda et al., 2007), optical scanning (Bacskai et al., 2003; Hintersteiner et al., 2005), and magnetic resonance imaging (MRI) (Higuchi et al., 2005), have enabled visualization of Aβ deposits in humans with AD and/or AD mouse models, and there has been a growing expectation that low-molecular-weight ligands for β-pleated sheet structures will also serve as molecular probes for tau amyloids. Although the majority of plaque-imaging agents used for clinical PET studies do not bind to tau lesions (Klunk et al., 2003), at least one radiolabeled β sheet ligand, [^{18}F]FDDNP, enables PET imaging of AD NFTs (Small et al., 2006). However, a relatively low contrast of in vitro autoradiographic and in vivo PET signals for [^{18}F]FDDNP putatively reflecting tau lesions does not allow a simple visual inspection of images for the assessment of tau pathologies in living subjects

(Small et al., 2006; Thompson et al., 2009). Thus, better tau radioligands with higher affinity for tau fibrils and/or less nonspecific binding to tissues are urgently needed to complement high-contrast senile plaque imaging agents, including widely studied [^{11}C]Pittsburgh Compound-B ([^{11}C]PIB) (Klunk et al., 2004) and United States Food and Drug Administration-approved [^{18}F]florbetapir (Yang et al., 2012). In addition, [^{18}F]FDDNP and several other candidate tau probes do not bind to tau inclusions in non-AD tauopathy brains without plaque deposition (Okamura et al., 2005) and therefore can be clinically characterized only in AD patients with comingled Aβ and tau amyloids. Hence, compounds that detect diverse tau aggregates, including tau inclusions in non-AD neurodegenerative diseases and tau Tg models, could be used to interrogate in vivo interactions between exogenous ligands and tau pathologies.

Here, we found that the lipophilicity of β sheet ligands is associated with their selectivity for tau versus Aβ fibrils and that the core dimensions of these chemicals are major determinants of their reactivity with a broad spectrum of tau aggregates in diverse tauopathies and mouse models of tau pathology. Building on these observations, we developed a series of fluorescent compounds capable of detecting diverse tau lesions using optical and PET imaging in living Tg mouse models of tauopathies. Finally, we identified a radiotracer that produced the highest contrast for tau inclusions in animal PET and used it in exploratory in vivo imaging studies of AD patients, providing clear demonstration of signal intensification in tau-rich regions, in sharp distinction to [^{11}C]PIB-PET data reflecting plaque deposition.

RESULTS

Identification of PBBs as Ligands for Diverse Tau Inclusions in Human Tauopathies

We screened an array of fluorescent chemicals capable of binding to β sheet conformations (see the Compounds subsection in the Experimental Procedures). Fluorescence labeling with these compounds were examined in sections of AD brains bearing Aβ and tau amyloids (Figures 1A and 2A) and non-AD tauopathy brains characterized by tau inclusions and few or no Aβ plaques (Figure 2). Amyloid PET tracers currently used for human PET studies, PIB (Klunk et al., 2004), and BF-227 (Kudo et al., 2007), tightly bound to senile plaques, while they only weakly reacted with AD NFTs (Figures 1A; Figure S1 available online). PET probes reported to selectively label tau aggregates, BF-158 (Okamura et al., 2005) and THK523 (Fodero-Tavoletti et al., 2011), detected AD NFTs (Figures 2A and S1) but microscopically detectable fluorescence signals produced by FDDNP, which are presumed to bind to both Aβ and tau fibrils (Small et al., 2006), were consistent with dense cores of classic plaques and distinct from tau lesions (Figures 2A and S1). None of the above-mentioned PET ligands were reactive with tau inclusions in non-AD tauopathies, such as Pick bodies in Pick's disease (Figures 2A and S1) and neuronal and glial fibrillary lesions in PSP and CBD (data not shown). By contrast, these pathologies were intensely labeled with a widely used amyloid dye, thioflavin-S, and a derivative of another classic amyloid dye Congo red, (E,E)-1-fluoro-2,5-bis(3-hydroxycarbonyl-4-hydroxy)styrylbenzene (FSB) (Higuchi et al., 2005; Maeda et al., 2007) (Figures 1, 2A, and S1), although these chemicals may not undergo efficient transfer through the blood-brain barrier (BBB) (Zhuang et al., 2001). Because compounds possessing a π-electron-conjugated backbone longer than 13Å exhibited affinities for pathological inclusions in a broad range of tauopathies, we examined binding of additional chemicals with a variety of structural dimensions to tau aggregates and found that affinity for non-AD tau inclusions could be attributed to a core structure with a specific extent ranging from 13 to 19 Å (Figure S1). Based on this view and the known fact that chemicals with a flat and slender backbone could pass through and attach to channel-like accesses in β-pleated sheets (Krebs et al., 2005), we developed a class of compounds, phenyl/pyridinyl-butadienyl-benzothiazoles/benzothiazoliums (PBBs), by stretching the core structure of a prototypical fluorescent amyloid dye, thioflavin-T, with two C = C double bond inserts between aniline (or aminopyridine) and benzothiazole (or benzothiazolium) groups (Figure 1B).

All PBB compounds intensely labeled NFTs, neuropil threads, and plaque neurites in AD brains (Figure 1C). Interestingly, the affinity of these PBBs for Aβ plaques lacking dense cores was positively correlated with their lipophilicity (Figure 1C), and thereby three potential probes with relatively low logP (log of the octanol/water partition coefficient) values, including PBB3, 2-[4-(4-methylaminophenyl)-1,3-butadienyl]-benzothiazol-5,6-diol (PBB4) and PBB5 (structurally identical to Styryl 7, CAS registry number 114720-33-1), appeared suitable for visualizing tau pathologies in living organisms with reasonable selectivity. High-affinity of PBBs for tau lesions was further demonstrated by fluorometric analyses using Aβ and tau filaments assembled in a test tube (Table S1; experimental procedures are given in the Supplemental Experimental Procedures), but the most and least lipophilic PBB members displayed similar selectivity for in vitro tau versus Aβ pathologies, implying a methodological limitation in screening chemicals for tau-selective ligands based on binding to synthetic peptides and recombinant proteins. PBBs and FSB were also shown to label tau inclusions in non-AD tauopathies, such as Pick's disease (Figures 2A and S1), PSP, and CBD (Figure 2B), all of which were immunodetected by an antibody specific for phosphorylated tau proteins (AT8).

In Vitro and Ex Vivo Fluorescence Imaging of Tau Lesions in Tau Tg Mice by PBBs

To obtain in vivo evidence of direct interaction between PBBs and tau lesions, we employed Tg mice expressing a single human four-repeat tau isoform with the P301S FTDP-17 mutation (PS19 line, see Figure S2 for neuropathological features of this Tg strain) (Yoshiyama et al., 2007). Similar to the findings in non-AD tauopathy brains, NFT-like inclusions in the brain stem and spinal cord of PS19 mice were clearly recognized by PBBs (Figures 3A and S1). We then performed ex vivo fluorescence labeling of tau lesions in PS19 mice with intravenously administered PBBs. Brains and spinal cords were removed 60 min after tracer injection, and fluorescence microscopy revealed an intense accumulation of these compounds in fibrillary tau inclusions abundantly seen throughout the sections by

A C

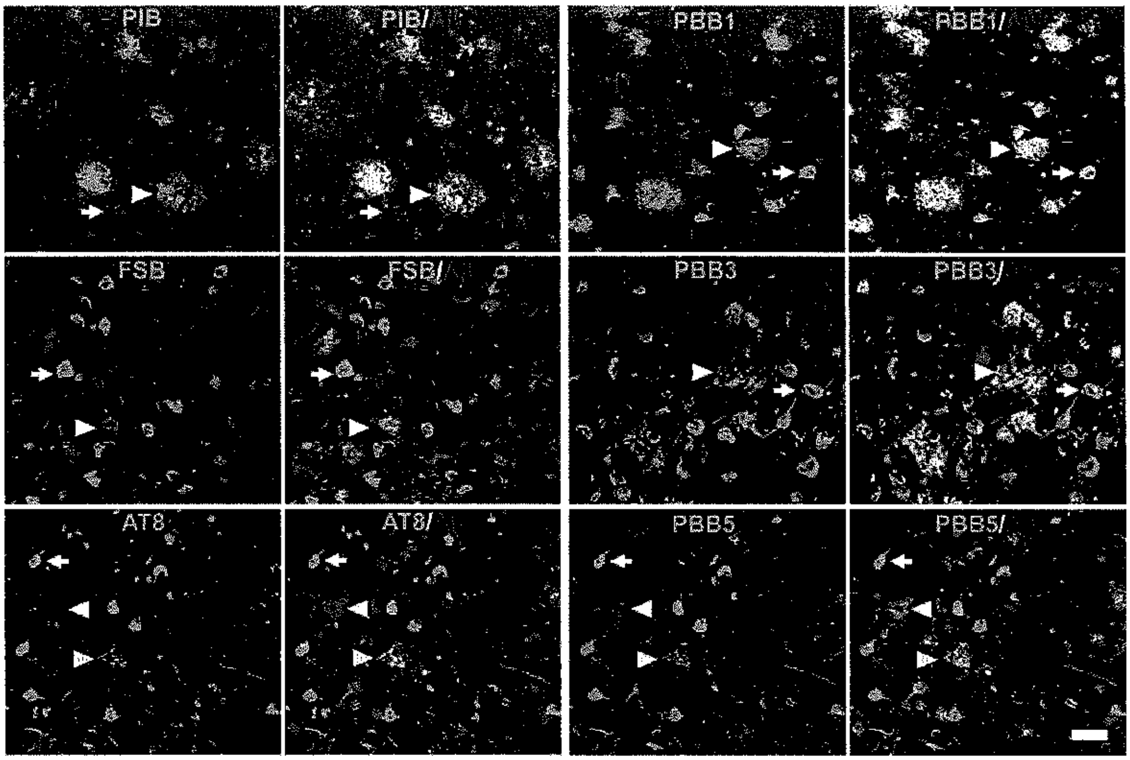

B

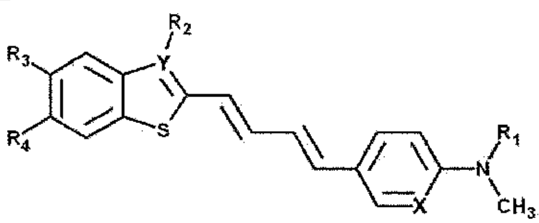

Compound	R_1	R_2	R_3	R_4	X	Y	ClogP
PBB1	CH_3	-	H	H	C(H)	N	5.44
PBB2	H	-	H	OH	C(H)	N	3.57
PBB3	H	-	H	OH	N	N	3.30
PBB4	H	-	OH	OH	C(H)	N	2.97
PBB5	CH_3	CH_3CH_2	H	H	C(H)	N^+	2.32

Figure 1. Design and Characterization of PBB Compounds as Potential Imaging Agents for Tauopathies
(A) Confocal fluorescence images of frontal cortex sections from an AD patient. Following fluorescence labeling (pseudocolors are converted to green) with PIB (top row) and FSB (middle row), the samples were immunostained with an antibody against AβN3(pE) (red in the right column). PIB intensely labeled Aβ plaques (white arrowheads) but did not clearly label NFTs (arrows). By contrast, NFTs and neuropil threads were intensely labeled by FSB, whereas the staining of diffuse plaques was negligible. A section was also doubly immunolabeled (bottom row) with AT8 (green) and anti-AβN3(pE) antibodies (red in the right panel), to demonstrate the abundance of tau and Aβ amyloids in this area. Yellow arrowheads indicate tau-positive dystrophic neurites associated with senile plaques.
(B) Structures of PBBs. Neutral benzothiazoles (PBB1-4) are newly synthesized chemicals, and a charged benzothiazolium, PBB5, is identical to a commercially available near-infrared laser dye.
(C) Confocal fluorescence images of PBBs (pseudocolors are converted to green) and AβN3(pE) (red in the right column) staining in sections adjacent to those displayed in (A). The intensity of plaque staining (arrowheads) relative to that of NFTs (arrows) was positively associated with the lipophilicity of PBBs. As compared with PBB1 (top row) staining, labeling of diffuse plaques with PBB3 (middle row) was substantially attenuated. PBB5 was nearly unreactive with diffuse plaques (bottom row), and subsequent double immunofluorescence staining of the same section (bottom row in C) illustrated good agreement of PBB5 labeling with the distribution of AT8-positive NFTs.
Scale bar, 50 μm (A and C). See also Figure S1 and Table S1.

staining with thioflavin-S, FSB, and AT8 (Figure 3B). On the other hand, no overt in vitro (Figure 3A) or ex vivo (data not shown) fluorescence of these ligands was noted in the corresponding regions of non-Tg wild-type (WT) mice. Consistent with these observations, two-photon laser scanning fluorescence microscopy of ex vivo samples demonstrated somatic and neuritic staining of a subset of tangle-bearing neurons with intravenously injected 2-[4-(4-methylaminophenyl)-1,3-butadienyl]-benzothiazol-6-ol (PBB2) and PBB4 in unsliced spinal cord blocks from PS19 mice (Figure 3B).

In Vivo Macroscopic and Mesoscopic Optical Detection of Fibrillar Tau Pathologies in a Mouse Model Using PBB5

We next characterized PBBs with the use of in vivo fluorescence imaging modalities, which permitted a quick assessment of

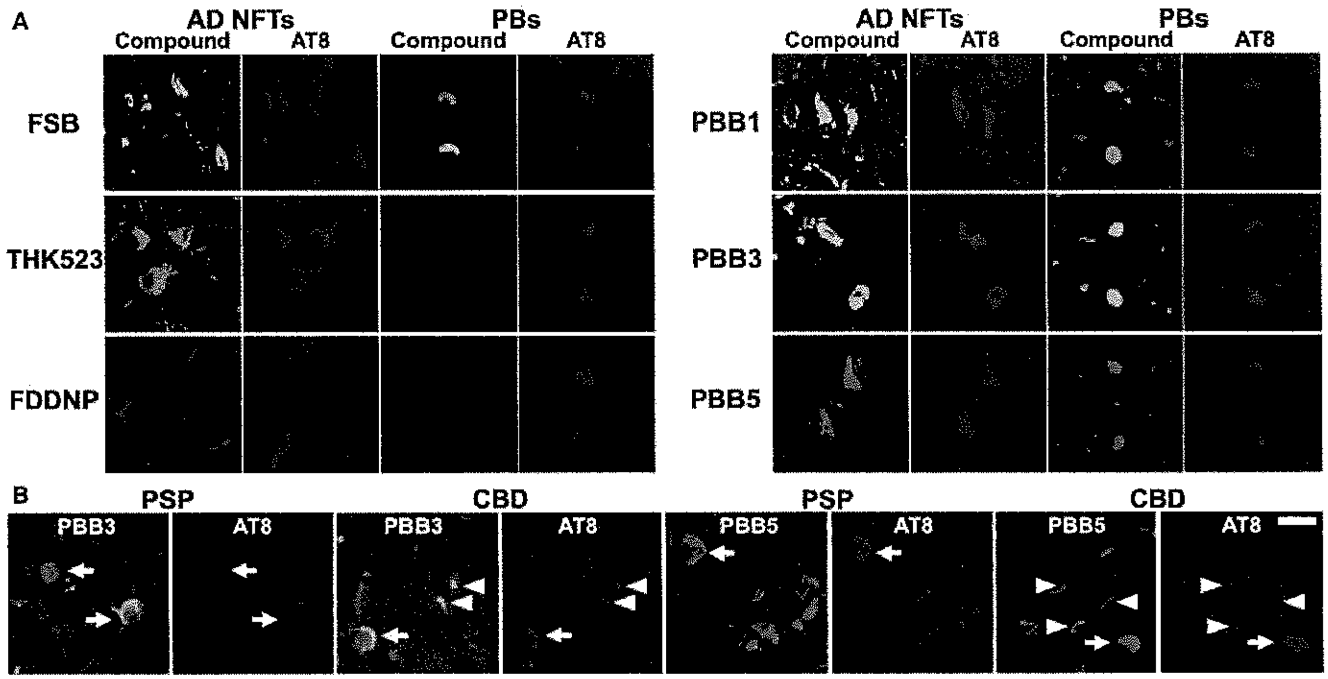

Figure 2. Binding of Tau Ligands to Tau Lesions in AD and Non-AD Tauopathy Brains

(A) Double fluorescence staining of AD NFTs and Pick bodies (PBs) in Pick's disease with PBBs, other tau ligands, and anti-phospho-tau antibody (AT8). FSB and PBBs sensitively captured AD NFTs and PBs. AD NFTs were labeled with THK523. Meanwhile, PBs were not visualized by these compounds. NFTs and PBs were barely recognizable by using FDDNP.

(B) Double fluorescence staining of neuronal tau inclusions (arrows) in PSP and CBD and putative astrocytic plaques (arrowheads) in CBD. A substantial portion of tau fibrils in neurons were captured by PBB3 and PBB5, but a much smaller subset of phosphorylated tau aggregates in astrocytic plaques were labeled with these compounds.

Scale bar, 20 μm (A and B). See also Figures S2 and S3.

candidate chemicals without the need for radiolabeling. Because PBB5 is fluorescent, with peak excitation and emission wavelengths in a near-infrared range (Table S1), this compound is applicable to in vivo optical imaging of tau deposits in laboratory animals. To examine this possibility, fluorescence images were obtained from living mice over a time course following intravenous PBB5 injections using a small animal-dedicated system permitting the intravital observation of fluorescence signals at magnifications varying between macroscopic and microscopic levels. Tail vein administration of PBB5 in PS19 mice revealed strong fluorescence relative to non-Tg WT mice in the central nervous system (CNS) above the slit between the base of the skull and first vertebra, through the skin and connective tissues overlaying the cisterna magna (Figures S3A–S3D), suggesting a concentration of this tracer in the PS19 spinal cord. In line with this in vivo observation, the hindbrain and spinal cord of PS19 mice, which were dissected out at 2 hr after the injection of PBB5, exhibited increased retention of this compound compared to non-Tg WT mice (Figures S3E–S3G).

In vivo optical imaging of tau Tg mice was subsequently performed using a device equipped with a pulsed diode laser and a photomultiplier tube to detect deep signals through the skull. Elevated levels of fluorescence intensity were found in homogenized brain stem samples collected from PS19 mice at 20 hr after the intravenous tracer administration (Figure S4A), indicating a long-lasting in vivo binding of PBB5 to tau fibrils. To support the ex vivo evidence, fluorescence intensity was noninvasively analyzed in living PS19 and non-Tg WT mice treated with PBB5. The mice, with their heads shaved in advance, were prescanned, and autofluorescence signals were detected at a relatively high level in an area corresponding to the frontal forebrain. Using these baseline signals as landmarks, regions of interest (ROIs) were defined in the frontal cortex, brain stem, and spinal cord (Figure 4A). The near-infrared fluorescence was notably increased immediately after the intravenous injection of PBB5 (Figure S4C), and the fluorescence in the brain stem and spinal cord ROIs of PS19 mice much exceeded that in WT mice at 30 min (Figure 4B). Fluorescence intensity in the frontal cortex ROI, normalized on the basis of integration time and laser power, was lower in PS19 mice than in WT mice over 120 min after tracer injection (Figure S4B), which may reflect impaired CNS delivery of the tracer in Tg mice due to degenerative changes (see Figures S4C–S4L for details), and thereafter this became almost equivalent between the two genotypes (Figure S4B). Meanwhile, persistent retention of the signals in the brain stem and spinal cord ROIs of PS19 mice was observed beyond 240 min (Figures 4B and S4B). A more quantitative index comparable among different mice was determined by calculating the target-to-frontal-cortex ratio of fluorescence intensity and was shown to increase over time particularly in PS19 mice (Figures 4C and 4D). This ratio was significantly greater in PS19 mice than in WT mice at 240 min (Figure 4E), beyond which the difference

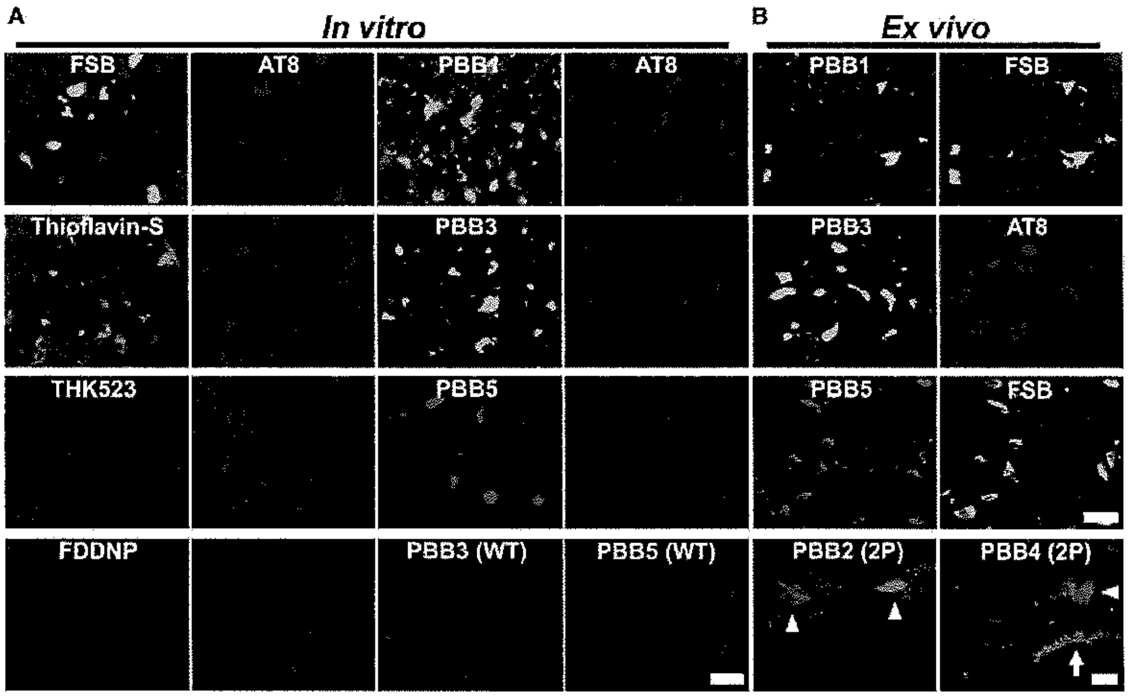

Figure 3. In Vitro and Ex Vivo Labeling of NFTs in PS19 Mice with PBB Compounds

(A) Double fluorescence staining of intraneuronal tau aggregates in postmortem brain stem slices of a 12-month-old PS19 mouse with PBB, other amyloid ligands, and anti-phospho-tau antibody (AT8).

(B) Binding of intravenously administered PBBs (0.1 mg/kg PBB5 and 1 mg/kg PBB1 and PBB3) to NFTs in PS19 mice at 10–12 months of age. The tissues were sampled at 60 min after tracer administration. The brain stem (top row) and spinal cord (second and third rows from the top) sections abundantly contained neurons showing strong fluorescence (left), and subsequent staining with FSB or AT8 (right) indicated that these cells were laden with tau amyloid fibrils (right). Putative intraneuronal tau inclusions in unsectioned spinal cords (arrowheads in the bottom row) removed from PS19 mice at 60 min after intravenous injection of PBB2 and PBB4 were also clearly visible by using a two-photon (2P) fluorescence microscopic system. Arrow in the bottom row indicates a cluster of auto-fluorescence signals from blood cells.

Scale bars, 25 μm (A), 30 μm (top to third rows in B), and 20 μm (bottom row in B).

between the two lines of mice became nearly constant (Figures 4C and 4D). The intensity ratio of the spinal cord ROI to the frontal cortex in PS19 mice at 240 min was also significantly correlated with the abundance of NFTs stained with FSB (Figure 4F), but such correlations were not statistically significant in the brain stem (Figure 4F), implying limitations of the intensitometry in some brain regions below the cerebellum and fourth ventricle.

Intravital Imaging of Individual Tau Inclusions by PBB3 and Two-Photon Laser Scanning Fluorescence Microscopy

Two-photon excitation microscopy, which enables optical sectioning, potentially up to 1 mm deep, in living tissues, could be utilized to visually demonstrate transfer of a fluorescent probe from the plasma compartment into the cytoplasm of CNS neurons and binding of the probe to intraneuronal tau inclusions. We therefore captured fluorescence signals from intravenously administered PBB3 by in vivo two-photon laser scanning microscopic imaging of the spinal cord of laminectomized PS19 mice. Within 3 s of PBB3 injection, green fluorescence signals emerged in blood vessels prelabeled with red with intraperitoneal treatment using sulforhodamine 101 and subsequently diffused from the vasculatures to the spinal cord parenchyma over the next few minutes (Figures 5A–5F). These diffuse signals declined thereafter due to the clearance of PBB3 from the tissue, whereas intense labeling of putative tau inclusions with green fluorescence appeared in a subpopulation of large cells morphologically identified as neurons at 3–5 min after PBB3 injection (Figures 5G and 5H). These intracellular PBB3 fluorescent signals were not found in the spinal cord of WT mice (Figure 5I). As the BBB of the brain and spinal cord are presumed to be identical, the two-photon microscopic data obtained here provide compelling evidence that PBB3 rapidly transits the BBB and neuronal plasma membranes, where it binds to intraneuronal tau inclusions. Accumulation of injected PBB3 in AT8-positive, NFT-like lesions of Tg mice was postmortemly confirmed by ex vivo microscopy (Figures 5J and 5K).

Autoradiographic and PET Imaging of Tau Lesions in PS19 Mice by Radiolabeled PBBs

We investigated the kinetic properties of PBBs by high-performance liquid chromatography (HPLC) analyses of plasma and brain samples collected from non-Tg WT mice treated with these ligands. Following intravenous administration, PBB5 was rapidly converted into a major metabolite, which at 5 min was found at high levels in both plasma and brain extracts. Subsequent liquid

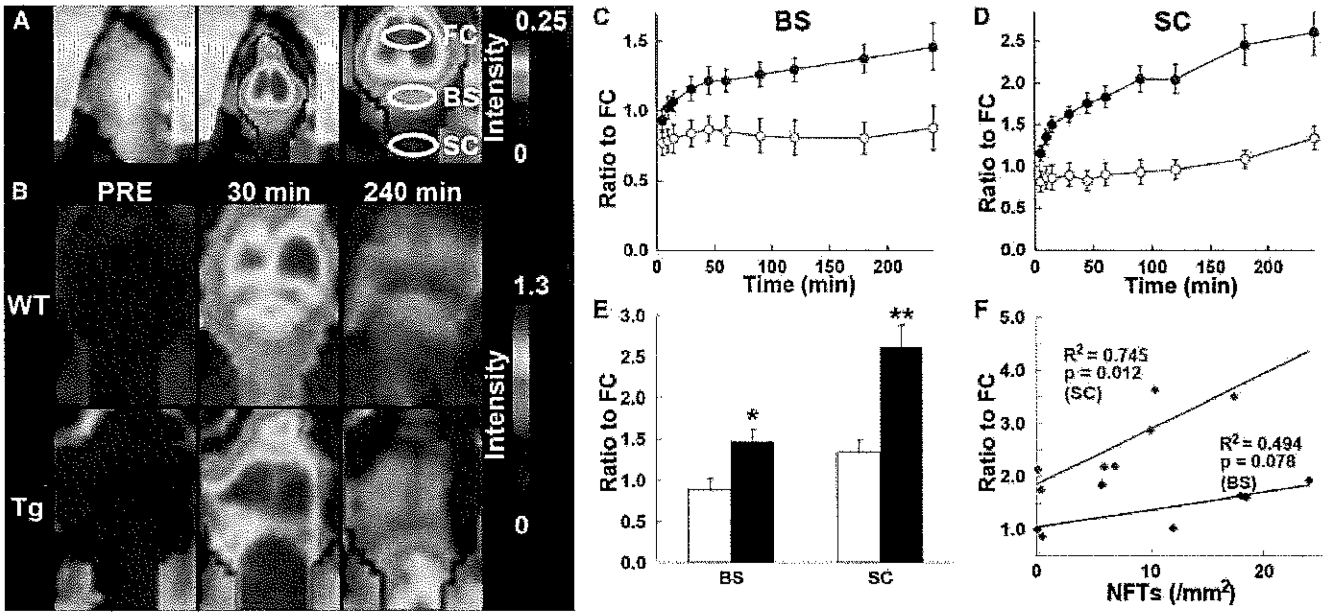

Figure 4. Noninvasive Near-Infrared Imaging of Tau Pathology in Living Tau Tg Mice Using Pulsed Laser Optics and PBB5

(A) Baseline autofluorescence signals (middle) are overlaid on the visible background image of a shaven non-Tg WT mouse head (left). Ellipsoidal ROIs are defined above the frontal cortex (FC), brain stem (BS), and cervical spinal cord (SC) guided by a relatively intense emission from the FC region (right).

(B) Fluorescence intensity maps in 12-month-old WT (top) and PS19 (Tg; bottom) mice before and at 30 and 240 min after the intravenous administration of PBB5 (0.1 mg/kg). The intensity maps (A and B) are normalized by the FC ROI value at 30 min after tracer injection. Long-lasting retention of the tracer was noted in the BS and SC ROIs of the Tg mouse.

(C and D) Target-to-FC ratios of fluorescence intensity in the BS (C) and SC (D) ROIs over the image acquisition time in the WT (open circles; n = 7) and PS19 (closed circles; n = 7) mice. There were significant main effects of time, region, and genotype in two-way, repeated-measures ANOVA (time, $F_{(11, 132)} = 17.6$, $p < 0.001$; region, $F_{(1, 12)} = 29.9$, $p < 0.001$; genotype, $F_{(1, 12)} = 23.6$, $p < 0.001$).

(E) Target-to-FC ratios in the BS and SC ROIs of the WT (open columns) and tau Tg (closed columns) mice at 240 min after tracer injection. *$p < 0.05$; **$p < 0.01$; two-way repeated-measures ANOVA with Bonferroni's post hoc analysis.

(F) Scatterplots of target-to-FC ratios at 240 min versus the number of FSB-positive NFTs per unit area of postmortem 20 μm tissue slices in BS (blue symbols) and SC (red symbols) ROIs of tau Tg mice. Solid lines represent regressions; p values were determined by t test. Vertical bars in the graphs represent SEs.

See also Figures S3 and S4.

chromatography-mass spectrometry (LC-MS) assays suggested that the major metabolite was likely a reduced, electrically neutralized derivative of PBB5 (Figures S5A and S5B). Besides transventricular uptake of unmetabolized PBB5 as implied above, this uncharged form incapable of emitting near-infrared light could readily penetrate the BBB, as well as cell membranes, and thereafter could be reoxidized into its original form, thereby enabling it to bind to tau fibrils, particularly at sites exposed to oxidative stress in pathological conditions. In addition, PBB4 was promptly converted to metabolites capable of entering the brain. Finally, studies of PBB2 and PBB3 showed that they exhibited reasonable biostability and sufficient entry into and clearance from the brain. Indeed, HPLC assays demonstrated that fractions of unmetabolized PBB2 and PBB3 in mouse plasma were 23.5% and 16.3%, respectively, at 3 min after intravenous administration and were 4.6% and 2.8%, respectively, at 30 min. There were also no metabolites of PBB2 and PBB3 detectable in the mouse brain at 3 and 30 min.

We then radiolabeled PBB2 and PBB3 with ^{11}C to conduct autoradiographic and PET assays using PS19 mice. In vitro autoradiography using frozen tissue sections showed binding of these radioligands to the brain stem of PS19 mice and neocortex of AD patients (Figure 6A). As expected from their lipophilicities, [^{11}C]PBB3 yielded high-contrast signals with less nonspecific labeling of myelin-rich white matter than did [^{11}C]PBB2, and the accumulation of [^{11}C]PBB3 in pathological regions was nearly completely abolished by the addition of nonradioactive compounds. Similarly, ex vivo autoradiographic studies demonstrated that intravenously administered [^{11}C]PBB3 selectively labeled the brain stem and spinal cord of PS19 mice harboring neuronal tau inclusions, whereas tau-associated [^{11}C]PBB2 radiosignals were less overt because of a considerable level of nonspecific background (Figure 6B; Figures S6C–S6F). Finally, in vivo visualization of tau lesions in PS19 mouse brains was enabled by a microPET system using these two tracers (Figures 6C, S6A, and S6B). Following intravenous injection, [^{11}C]PBB3 rapidly crossed the BBB and unbound and nonspecifically bound tracers were promptly washed out from the brain with a half-life of ~10 min (left panel in Figure 6E). The retention of [^{11}C]PBB3 signals in the brain stem of 12-month-old PS19 mice lasted over the imaging time (90 min), producing a pronounced difference from that in age-matched non-Tg WT mice (left panel in Figure 6E). By selecting the striatum as a reference region lacking tau deposits, the target-to-reference ratio was estimated for the brain stem, with the value in PS19 mice peaking at around 70 min, contrasting with its continuous decrease over

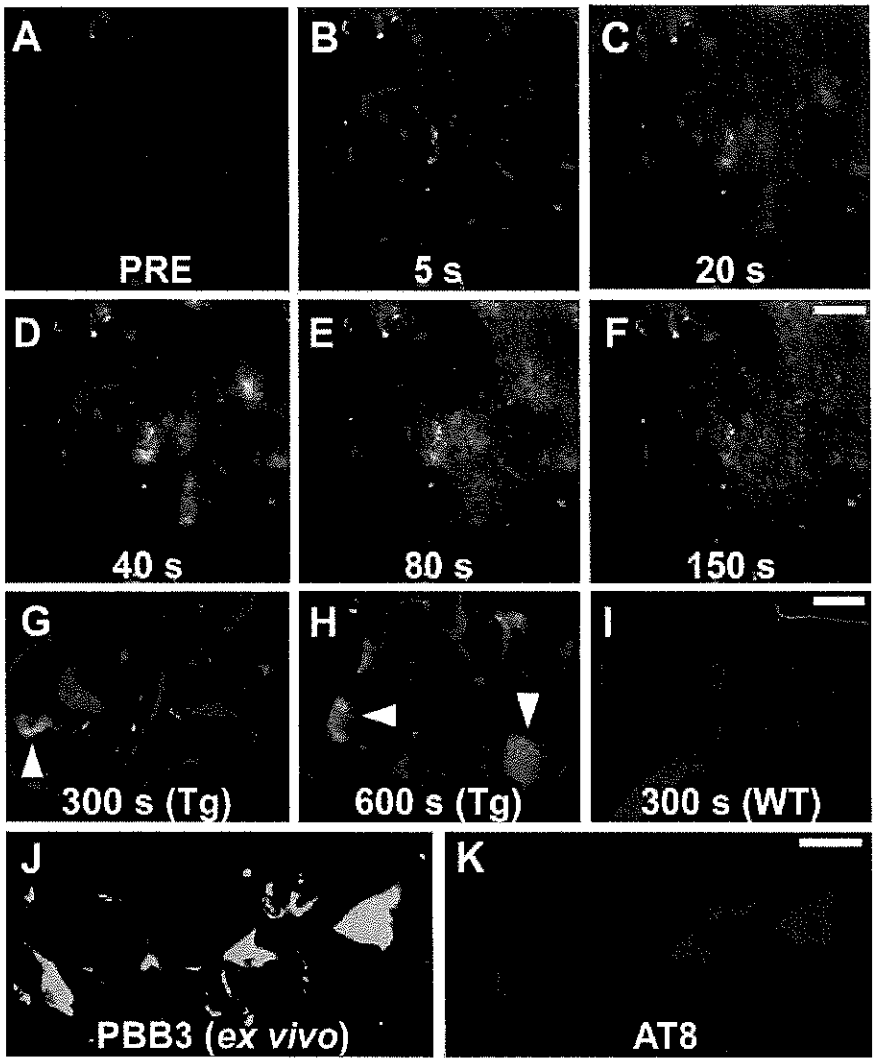

Figure 5. Real-Time Two-Photon Laser Scanning Images of PBB3 Diffusing from Vessels, Binding to Intraneuronal Tau Inclusions, and Clearing from Spinal Cord

(A–H) A maximum projection of fluorescence in a 3D volume of the spinal cord of a living PS19 mouse at 12 months of age before (A) and at various time points after (B–H) intravenous administration of PBB3 (1 mg/kg). Blood vessels were labeled with sulforhodamine 101 (red) intraperitoneally injected at 15 min before PBB3 administration. Green fluorescence indicates a rapid transfer of PBB3 from the plasma to tissue parenchyma (B–E) and subsequent washout from the tissue (F). Background PBB3 signals were further attenuated beyond 300 s, whereas somatodendritic labeling by this compound was observed in a subset of neurons (arrowheads in G and H).

(I) Fluorescence image of WT spinal cord at 300 s after PBB3 injection demonstrates no overt retention of the tracer in the tissue.

(J and K) Ex vivo microscopy for a brain stem section of the same Tg mouse. Tissues were obtained at 60 min after PBB3 injection. Signals of intravenously administered PBB3 (J) overlapped with AT8 immunoreactivity (K).

Scale bars, 50 μm (A–F), 25 μm (G–I), and 25 μm (J and K).

60 min in WT mice (right panel in Figure 6E). The mean ratio at 45–90 min was increased by 40% in 12-month-old PS19 mice as compared with age-matched WT mice ($p < 0.01$ by t test). The agreement between localizations of PET signals and tau inclusions in PS19 mice was proven by postmortem FSB staining of brain sections from scanned mice (Figure 6D). Significantly, the mean target-to-reference ratio in the brain stem quantified by PET correlated closely with the number of FSB-positive inclusions per brain section in the same region of the postmortem sample ($p < 0.001$ by t test; data not shown). [^{11}C]PBB2 exhibited slower clearance from the brain and higher nonspecific retention in myelin-rich regions than [^{11}C]PBB3 (Figure S6G), resulting in insufficient contrast of tau-bound tracers in the brain stem of PS19 mice and a small difference in the target-to-reference ratio of radioactivities between PS19 and WT mice (8% at 45–90 min; $p < 0.05$ by t test; Figure S6H) relative to those achieved with [^{11}C]PBB3.

As radiolabeling at the dimethylamino group in PBB5 with ^{11}C was unsuccessful, ^{11}C-methylation of a hydroxyl derivative of this compound was performed, leading to the production of [^{11}C]methoxy-PBB5 ([^{11}C]mPBB5; Figure S5C). PET images demonstrated complex pharmacokinetics of [^{11}C]mPBB5 (Figures S5D and S5E), and the difference in the specific radioligand binding between Tg and WT mice was small relative to the [^{11}C]PBB3-PET data (Figure S5F). After taking all of these findings into consideration, [^{11}C]PBB3 was selected as the most suitable ligand for in vivo PET imaging of tau pathology in tau Tg mice and human subjects.

Notably, the hippocampus of many PS19 mice was devoid of overt [^{11}C]PBB3 retention (Figure 6C), although a pronounced hippocampal atrophy was noted in these animals. This finding is in agreement with the well-known neuropathological features of PS19 mice in the hippocampus, because the accumulation of AT8-positive phosphorylated tau inclusions results in the degeneration of the affected hippocampal neurons prior to or immediately after NFT formation, followed by the clearance of their preNFTs or NFTs that are externalized into the interstitial CNS compartment (Figure S2). To explore the feasibility of our imaging agents in studies with other tauopathy model mice, we also performed fluorescence labeling with PBBs for brain sections generated from rTg4510 mice (Santacruz et al., 2005; the Supplemental Experimental Procedures). As reported elsewhere (Santacruz et al., 2005), these mice developed numerous thioflavin-S-positive neuronal tau inclusions in the neocortex and hippocampus, and reactivity of these lesions with PBBs was demonstrated by in vitro and ex vivo fluorescence imaging (Figure S7).

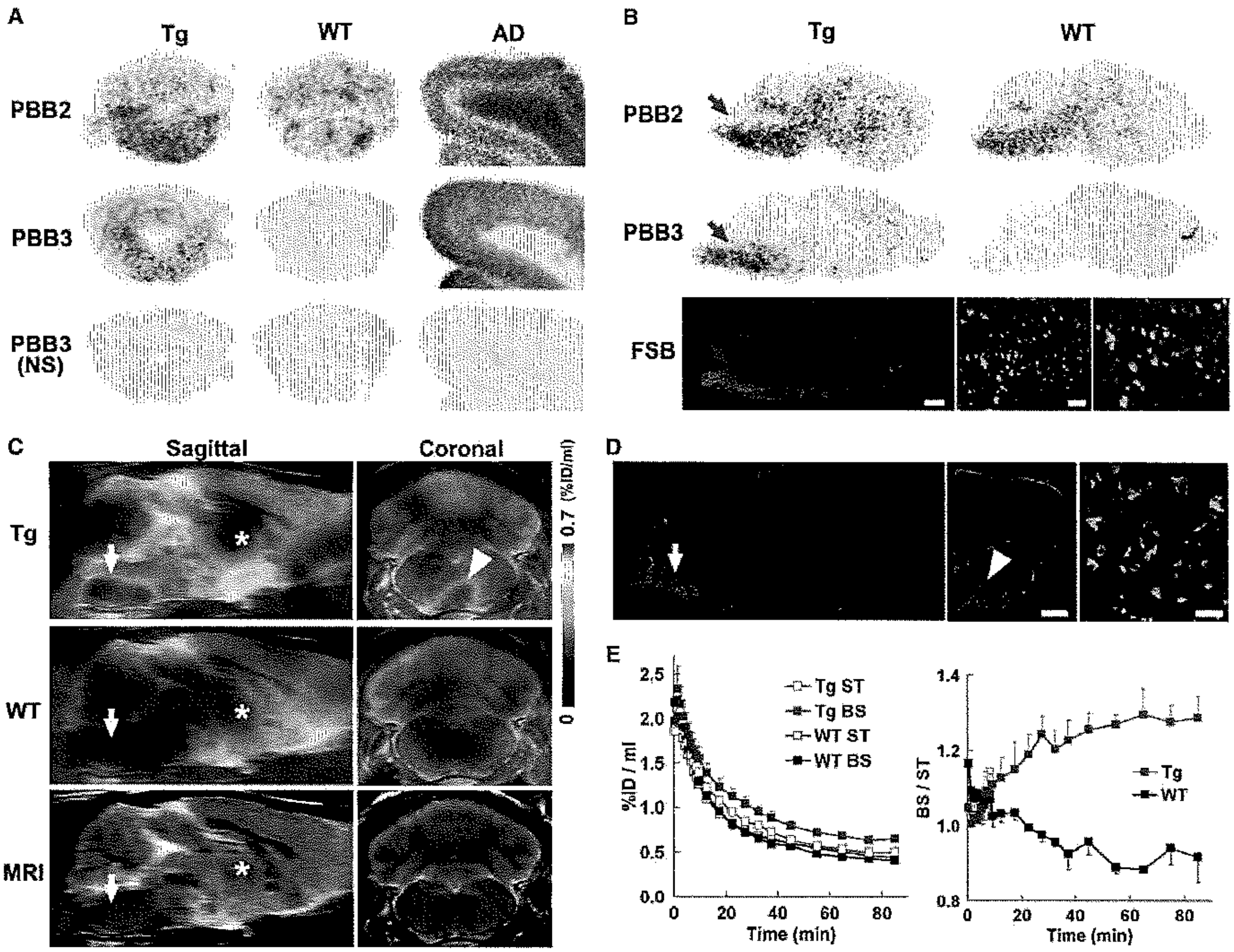

Figure 6. PET and Autoradiographic Detection of Tau Pathologies in PS19 Mice Using [^{11}C]PBB2 and [^{11}C]PBB3

(A) In vitro autoradiograms of PS19 and non-Tg WT hindbrains (coronal sections) and AD frontal cortex. Fibrillar aggregates in the mouse brain stem and AD gray matter produced intense radiolabeling with both tracers, but nonspecific background signals were also observed at a considerably high level with the use of [^{11}C]PBB2. Binding of [^{11}C]PBB3 was profoundly abolished by the addition of nonradioactive PBB3 (10 μM).

(B) Autoradiographic labeling with intravenously injected [^{11}C]PBB2 and [^{11}C]PBB3 in PS19 (Tg) and WT mice. The brains were removed at 45 min after injection and were cut into sagittal slices. The autoradiographic section of PS19 brain was also stained with FSB. Arrows indicate the brain stem containing numerous tau inclusions displayed at intermediate and high magnifications.

(C) Sagittal and coronal PET images generated by averaging dynamic scan data at 60–90 min after intravenous administration of [^{11}C]PBB3. The images are overlaid on the MRI template (images of the template alone are presented at the bottom). Arrows and asterisks indicate the brain stem and striatum, respectively, and arrowhead denotes intense radiolabeling in the medial brain stem of the PS19 mouse.

(D) FSB staining of PS19 mouse brain shown in (C). Sagittal (left) and coronal (middle) images and a high-power view of fibrillar inclusions (right) are displayed. Corresponding to high-level retention of [^{11}C]PBB3 in PET scans, abundant FSB-positive lesions were found in the medial brain stem (arrow and arrowhead).

(E) Time-radioactivity curves (left) in the striatum (ST) and brain stem (BS) and BS-to-ST ratio of radioactivity (right) over the imaging time in PS19 (Tg; red symbols) and WT (black symbols) mice ($n = 5$ each). Vertical bars in the graphs denote SEs.

Scale bars, 1 cm (A and B, top, middle, and bottom left panels); 1 cm (C and D, left and middle panels); 100 μm (B, bottom middle panel); and 100 μm (B, bottom right panel and D, right panel). See also Figures S5, S6, and S7.

Detection of Tau Pathologies in Living Brains of AD Patients by Comparative PET Imaging with [^{11}C]PBB3 and [^{11}C]PIB

In order to compare the bindings of [^{11}C]PBB3 and [^{11}C]PIB to tau-rich regions in the human brain, in vitro autoradiography was carried out with sections of AD and control hippocampus. A notable difference in labeling between these two radioligands was observed in the CA1 sector and subiculum of the AD hippocampus, where fibrillar tau aggregates predominantly localized to NFTs and neuropil threads (Figure 7A).

We subsequently conducted an exploratory clinical PET study for patients with probable AD ($n = 3$) and age-matched cognitively normal control (NC) subjects ($n = 3$). All AD patients exhibited a marked increase in the retention of [^{11}C]PIB in

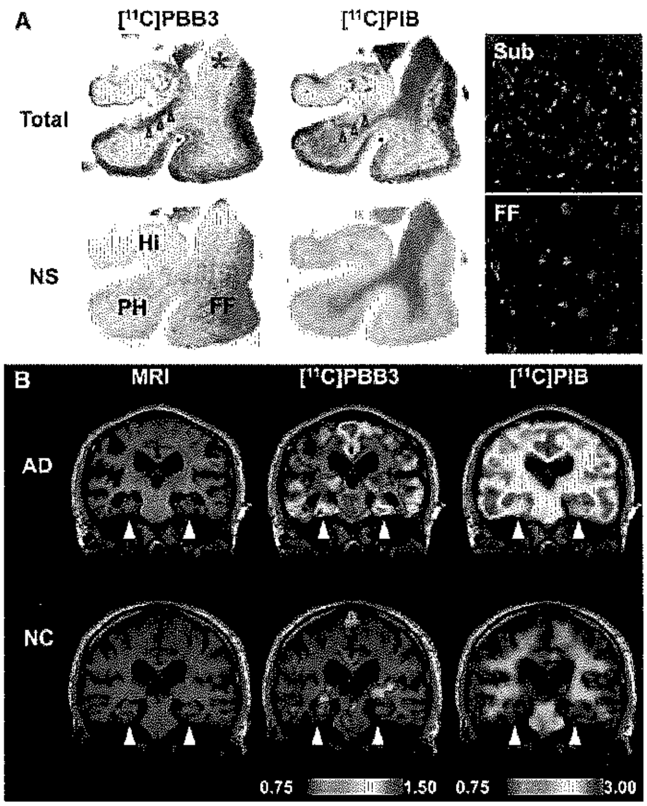

Figure 7. Accumulation of [^{11}C]PBB3 in the Hippocampal Formation of AD Patients Revealed by In Vitro Autoradiography and In Vivo PET

(A) Autoradiographic labeling of adjacent brain sections from an AD patient with 10 nM of [^{11}C]PBB3 (left) and [^{11}C]PIB (middle). The slices contain the hippocampus (Hi), parahippocampal gyrus (PH), fusiform gyrus (FF), and white matter (asterisks). Total binding (top) of [^{11}C]PBB3 and [^{11}C]PIB was markedly abolished (bottom) by addition of nonradioactive PBB5 (100 μM) and thioflavin-S (10 μM), respectively, except for the nonspecific (NS) labeling of white matter with [^{11}C]PIB. The hippocampal CA1 sector and subiculum displayed intense [^{11}C]PBB3 signals without noticeable binding of [^{11}C]PIB, and binding of [^{11}C]PBB3 in cortical areas flanking the collateral sulcus (identified by a red dot) and hippocampal CA2 sector (arrows) was also abundant relative to that of [^{11}C]PIB. FSB staining of amyloid fibrils in the sections used for autoradiography indicated the predominance of NFTs and diffuse plaques in the hippocampal subiculum (Sub) and fusiform gyrus (FF), respectively (right panels), supporting the strong reactivity of [^{11}C]PBB3 with AD NFTs.

(B) MRI (left) and PET imaging with [^{11}C]PBB3 (middle) and [^{11}C]PIB (right) performed in the same AD (top) and normal control (NC; bottom) subjects. Coronal images containing the hippocampal formation (arrowheads) are displayed. [^{11}C]PBB3- and [^{11}C]PIB-PET images were generated by estimating SUVRs at 30–70 min and 50–70 min after radiotracer injection, respectively, and were superimposed on individual MRI data. In the hippocampal formation, prominently increased retention of [^{11}C]PBB3 in the AD patient was in sharp contrast to the modest or negligible changes in [^{11}C]PIB binding as compared with NC. Scale ranges for SUVRs were 0.75–1.50 ([^{11}C]PBB3) and 0.75–3.00 ([^{11}C]PIB).

See also Figure S9.

plaque-rich areas, and all NC were negative for this PET assay. These subjects then received a [^{11}C]PBB3-PET scan, and the [^{11}C]PIB and [^{11}C]PBB3 images were compared in the same individuals. Intravenously injected [^{11}C]PBB3 was delivered to the brain tissue despite its relatively rapid metabolism in humans (Figures 9A and 9B). Unlike [^{11}C]PIB, [^{11}C]PBB3 showed minimal nonspecific binding to white matter and other anatomical structures with high myelin content, although it accumulated in dural venous sinuses in control and AD brains (Figures 7B, 8, and 9B). Time courses of regional radioactivity (Figures 9C and 9D; Figures S8A and S8B) and the standardized uptake value ratio (SUVR) to the cerebellum (Figures S8C and S8D) demonstrated accumulation of [^{11}C]PBB3 in several brain regions of AD patients as compared to controls (definition of these VOIs is indicated in Figure S8E). In agreement with autoradiographic findings, binding of [^{11}C]PBB3 to the medial temporal region, including the hippocampus, contrasted strikingly with the low-level retention of [^{11}C]PIB in this area (Figure 7B). There was a slight increase in the retention of [^{11}C]PBB3 primarily in the medial temporal region of a control subject with a loss of several points in Mini-Mental State Examination (MMSE) (subject 3 in Figure 8), appearing similar to the tau pathology at Braak stage III/IV or earlier (Braak and Braak, 1991), distinct from the lack of enhanced [^{11}C]PIB signals. Indeed, mild increase of medial temporal SUVR (Figure 9E) contrasted with unremarkable change in lateral temporal and frontal SUVRs in this subject (Figures 9G and 9H). Signals of [^{11}C]PBB3 were also intense mainly in the limbic region of a subject with early AD (subject 4 in Figure 8), but profound and moderate increases of SUVRs were also observed in the lateral temporal and frontal cortices, respectively, of this case (Figures 9G and 9H), resembling the localization of tau deposits at Braak stage V/VI (Braak and Braak, 1991). With the further cognitive decline as scored by MMSE (subjects 5 and 6 in Figure 8), additional increase in the retention of [^{11}C]PBB3 was found in the medial temporal region, precuneus, and frontal cortex (Figures 9E, 9F, and 9H). Meanwhile, a substantial decline of [^{11}C]PBB3 binding was noted in the lateral temporal cortex of subject 6 (Figures 8 and 9G). The SUVRs in the medial temporal region, precuneus, and frontal cortex were consequently well correlated with the decline of MMSE scores (Figures 9E, 9F, and 9H). In distinction with [^{11}C]PBB3-PET data, there was no overt association between the binding of [^{11}C]PIB and disease severity in AD patients (Figure 8), consistent with previous observations. These data support the potential utility of [^{11}C]PBB3 for clarifying correlations between the distribution of tau deposition and the symptomatic progression of AD.

As in vitro fluorescence staining indicated that PBB3 was reactive with not only tau lesions but also several types of senile plaques, particularly dense core plaques, density of binding sites, and affinity of [^{11}C]PBB3 for these sites were quantified by autoradiographic binding assays with hippocampal and neocortical sections of AD brains enriched with NFTs and senile plaques, respectively. These analyses demonstrated that specific radioligand binding sites were primarily constituted by high-affinity, low-capacity binding components in NFT-rich regions and low-affinity, high-capacity binding components in plaque-rich regions (Figures S9A and S9B). A subsequent simulation for radioligand binding in an area containing these two types of binding sites at a ratio of 1:1 indicated that the selectivity of [^{11}C]PBB3 for NFTs versus plaques may be inversely associated with concentration of free radioligands (Figure S9C). In a range of free concentration in the brain achievable

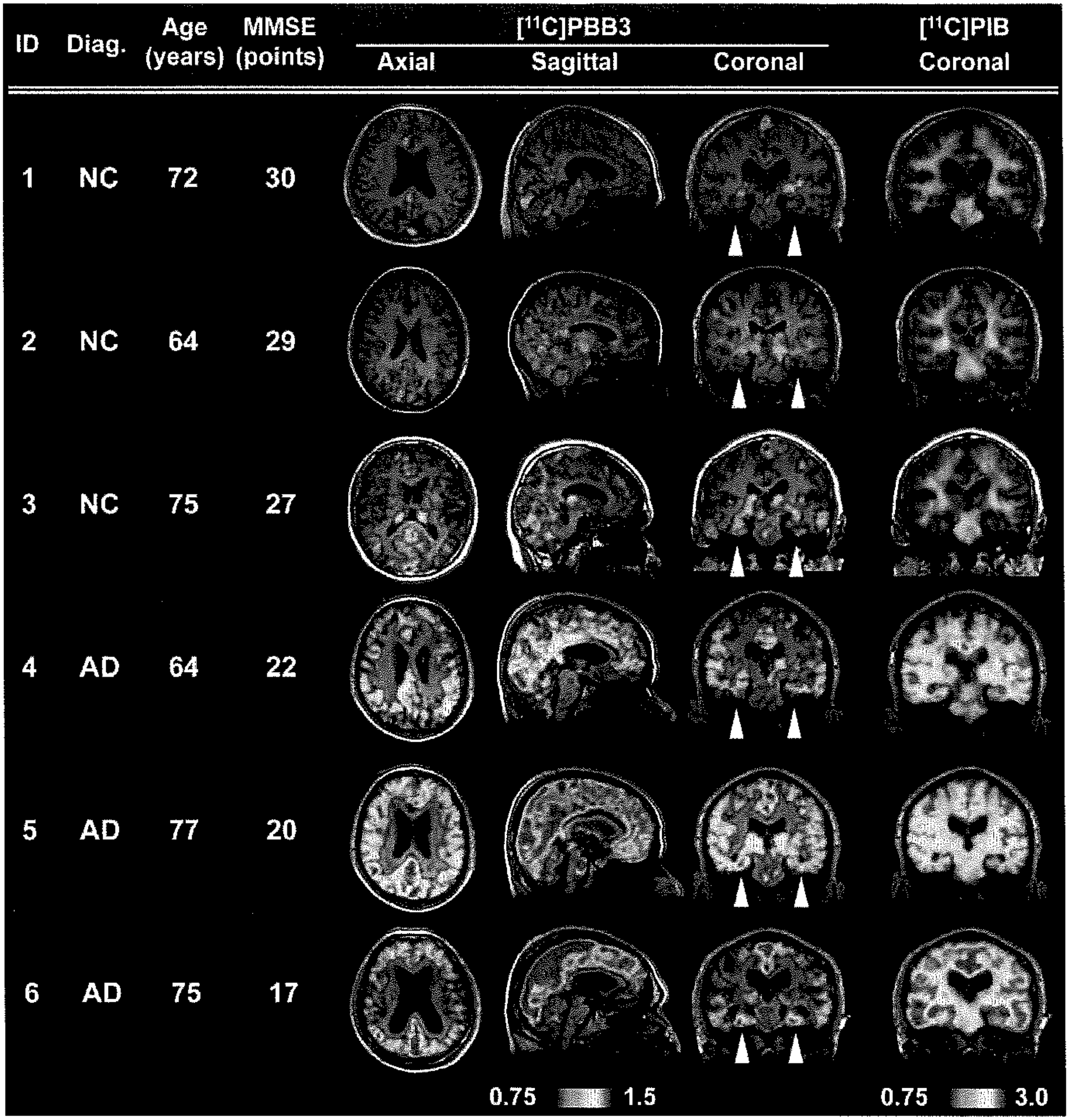

Figure 8. Orthogonal [^{11}C]PBB3-PET Images in All Human Subjects Examined in the Present Exploratory Clinical Study

Data are displayed as parametric maps for SUVR. The [^{11}C]PBB3 binding to the hippocampal formation (arrowheads) was increased consistently in AD patients in contrast to minimum radiotracer retention in normal control (NC) subjects with MMSE scores of 29–30 points (subjects 1 and 2). Another NC subject with an MMSE score of 27 points (subject 3) was negative for [^{11}C]PIB-PET but exhibited slight accumulation of radiotracer signals primarily around the hippocampus, resembling fibrillar tau deposition at Braak stage III/IV or earlier. Sagittal slices around the midline illustrate that radioligand signals were the most intense in the limbic system but began to expand to the neocortex in a patient with the mildest AD (subject 4), in agreement with the tau pathology at Braak stage V/VI, and was further intensified in most neocortical areas, corresponding to Braak stage VI, apparently as a function of the disease severity assessed by MMSE (subjects 5 and 6). The AD patient with the lowest MMSE score (subject 6) displayed a less profound increase of [^{11}C]PBB3 retention in the lateral temporal and parietal cortices than did the other two AD cases, and this is attributable to marked cortical atrophy in this individual and/or toxic loss of tau-bearing neurons in these brain areas at an advanced pathological stage. In contrast to the spatial profiles of [^{11}C]PBB3 binding, the distribution of [^{11}C]PIB signals appeared unchanged among AD subjects. See also Figure S9.

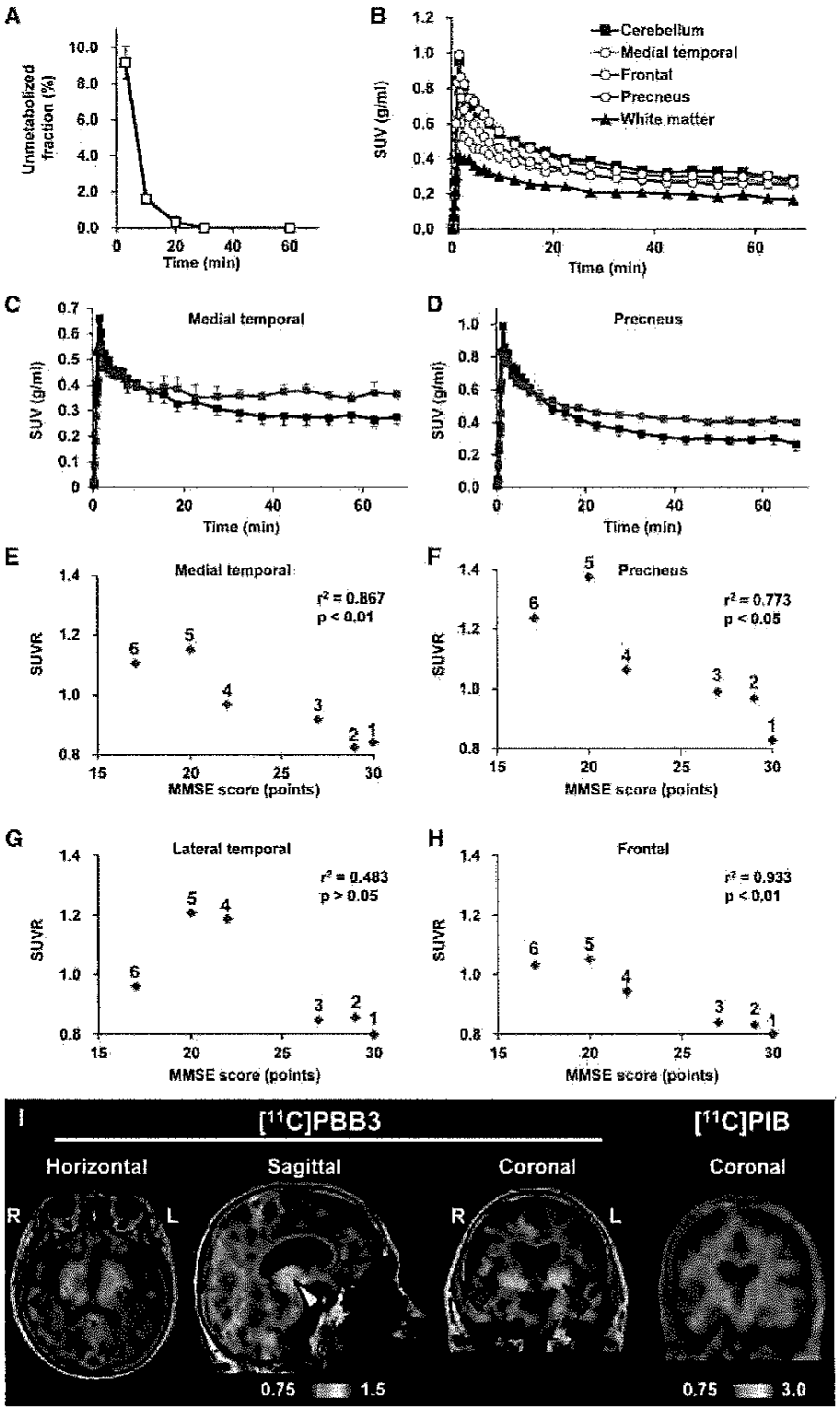

Figure 9. Pharmacokinetic Profiles of [^{11}C]PBB3 Administered to Humans and PET Images of a Patient Clinically Diagnosed as Having Corticobasal Syndrome

(A) Time course of unmetabolized [^{11}C]PBB3 fraction in plasma following intravenous radiotracer injection. The plot was generated by averaging data from six individuals.

(B) Time-radioactivity curves in different brain regions of cognitively normal control subjects over 70 min after intravenous injection of [^{11}C]PBB3. Data were generated by averaging values in two individuals and are presented as standard uptake values (SUVs).

(C and D) Comparisons of time-radioactivity curves in the medial temporal region (C) and precuneus (D) of normal controls (black symbols and lines; n = 3) and AD patients (red symbols and lines; n = 3).

(E–H) Scatterplots illustrating correlation of SUVRs with MMSE scores in the medial temporal region (E), precuneus (F), and lateral temporal (G) and frontal (H) cortices. Numbers beside symbols denote subject ID as indicated in Figure 8. Coefficients of determination (r^2) and p values by t test are displayed in graphs.

(I) [^{11}C]PBB3- and [^{11}C]PIB-PET images in a subject with clinical diagnosis of corticobasal syndrome. Images were generated as in Figures 7 and 8. Accumulation of [^{11}C]PBB3 was noticeable in the basal ganglia (red arrowheads) with right-side dominance and an area containing the thalamus and midbrain (yellow arrowhead).

Vertical bars in the graphs represent SEs. See also Figures S8 and S9.

at a pseudoequilibrium state in human PET imaging (<0.2 nM), [^{11}C]PBB3 is presumed to preferentially bind to tau lesions relative to in vitro autoradiographic (~1 nM) and fluorescence (>100 nM) labeling.

We also estimated contribution of [^{11}C]PBB3 bound to dense core plaques to total radiosignals in the neocortical gray matter of AD patients, by conducting autoradiography and FSB histochemistry for the same sections. Radiolabeling associated with dense cored plaques accounted for less than 1% and 3% of total gray matter signals in the temporal cortex and precuneus, respectively (Figures S9D–S9H). Moreover, fluorescence labeling of adjacent sections with PBB3 demonstrated that approximately 2% and 5% of total gray matter fluorescence signals were attributable to PBB3 bound to dense core plaques in the temporal cortex and precuneus, respectively. Hence, dense cored plaques were conceived to be rather minor sources of binding sites for [^{11}C]PBB3.

Finally, PET scans with [^{11}C]PBB3 and [^{11}C]PIB were conducted for a subject clinically diagnosed as having corticobasal syndrome. Retention of [^{11}C]PIB stayed at a control level, but notable accumulation of [^{11}C]PBB3 was observed in the neocortex and subcortical structures (Figure 9I), providing evidence for in vivo detection of tau lesions in plaque-negative

tauopathies. Interestingly, right-side dominant [^{11}C]PBB3-PET signals in the basal ganglia were consistent with laterality of atrophy in this area (Figure S8F). These findings may also be associated with a right-side dominant decrease in cerebral blood flow and left-side dominant motor signs in this patient.

DISCUSSION

Here, we report our efforts to develop BBB-penetrant ligands that are capable of binding to and visualizing intracellular tau aggregates in AD and non-AD tauopathies. These compounds may accordingly be useful for the differential diagnosis of neurological conditions in elderly subjects on the basis of the distribution of tau lesions, thereby opening up novel avenues for research in elucidating mechanisms of tau-mediated neurodegeneration, as well as tau-focused biomarkers and therapies.

Despite numerous efforts to develop imaging ligands to visualize tau pathologies in the brains of patients with AD and related tauopathies, the urgent need for these tau biomarkers remains largely unmet. To address this significant challenge, we also took advantage of a multimodal imaging system, which facilitates a quick and label-free validation of candidate compounds in terms of their transfer to the brain and retention in tau-rich regions. In addition, subcellular-resolution imaging optics exemplified by two-photon laser scanning microscopy provided proof of the rapid transfer of intravenously administered potential tau pathology imaging agents from plasma to the CNS extracellular matrix and subsequently to the cytoplasm of neurons, where they can bind to intracellular tau inclusions. Based on these encouraging preliminary data using nonlabeled compounds, a subset of these compounds was radiolabeled for use in PET imaging of Tg mice that model tau pathology, and a radioligand that yielded the best visualization of tau lesions in these Tg mice was selected for further testing in human AD patients and NC subjects as well as patients with probable CBD. This stepwise strategy enabled us to identify and advance the most promising PET probe for the visualization and quantitative assessment of tau pathology in the CNS of living human subjects. Interestingly, another research group has recently reported development of ^{18}F-labeled PET ligands for tau lesions mostly through assessments of binding to brain tissues, but not recombinant tau assemblies (Zhang et al., 2012; Chien et al., 2013), as in the present approach. These radioligands have been implied to produce considerably high contrasts for tau pathologies in living AD brains, and relatively long radioactive half-life of ^{18}F would enable delivery of radioligands from a radiosynthesis sites to multiple PET facilities. [^{11}C]PBB3 has distinct advantages over these compounds, as exemplified by affinity for diverse tau lesions, including Tg mouse tau aggregates, applicability to multimodal imaging, and induction of smaller radioactive exposure than ^{18}F-labeled ligands.

In the present work, we clinically validated the performance of [^{11}C]PBB3 as a tau imaging agent by comparing the distribution of [^{11}C]PBB3 with that of [^{11}C]PIB in AD brains. Tau deposits in patients with moderate or severe AD are thought to be distributed extensively in the neocortical and limbic regions (classified as Braak stage V/VI) (Braak and Braak, 1991), thereby resembling localization of senile plaques, except for the predominance of tau aggregates in the hippocampal formation. This rationalizes the use of radioactivity in the medial temporal area as an index to validate an imaging probe for tau pathology versus Aβ deposits in AD patients from prodromal to advanced stages. Furthermore, our preliminary data suggest that [^{11}C]PBB3 may be capable of capturing the temporospatial spreading of neurofibrillary tau pathologies from the limbic system (Braak stage III/IV or earlier) to neocortical areas (Braak stage V/VI) with the progression of AD (Figure 8). A considerable subset of tau lesions at Braak stage I/II is composed of phosphorylated tau deposits barely reactive with thioflavin-S (i.e., pretangles), and NFTs are relatively low in number and are confined to the transentorhinal cortex (Braak and Braak, 1991; Braak et al., 2011). Therefore, detection of these early tau pathologies would be more difficult. Our next-stage clinical study with expanded sample size and wider range of MMSE scores is currently ongoing to pursue tau accumulation in normal controls and subjects with mild cognitive impairments and AD at diverse stages and will bring more compelling insights into the significance of tau PET imaging in early diagnosis and prediction of AD. In addition, alterations of [^{11}C]PBB3 retention were indicated in the transition from mild to moderate AD. Loss of PET signals in the lateral temporal cortex of a patient with moderate AD (subject 6 in Figure 8) might not result from atrophy of this region, as the hippocampus of the same subject exhibited strong [^{11}C]PBB3 binding despite marked atrophy. Possible explanations for this change include formation of extracellular NFTs and their envelopment by astrocytes in the degenerating neocortex, profoundly modifying accessibility of these NFTs to exogenous molecules (Schmidt et al., 1988). This notion would need to be examined by combined autoradiogarphic and immunohistochemical assays of different brain regions.

Being able to visualize tau deposits with [^{11}C]PBB3 in non-AD tauopathies, such as PSP, CBD, and related disorders, is also of major importance, as suggested in the present PET data the support detectability of tau deposition in living CBD brains. As compared with NFTs and neuropil threads in AD, abundant tau deposits are largely confined to specific neuroanatomical locations of the CNS in tau-positive, plaque-negative illnesses, as exemplified by PSP and CBD (Dickson et al., 2011), but the homogenous and low-level background signals of [11C]PBB3 in brain parenchyma indicate the possibility of detecting tau lesions in these disorders. Following such in vivo assessments, a postmortem neuropathological evaluation of scanned subjects would be required as a reference standard for PET assays of non-AD tau pathologies.

[^{11}C]PIB-positive plaque formation nearly plateaus prior to the progression of brain atrophy in AD (Engler et al., 2006), but tau abnormalities may bridge the chasm between Aβ fibrillogenesis and neuronal death. Consistent with this notion, our PET/MRI data indicate that the deposition of tau inclusions as visualized by the intense [^{11}C]PBB3 labeling but lacking overt [^{11}C]PIB binding is closely associated with a local volume reduction in the hippocampal formation. Indeed, our pilot clinical PET study demonstrated that localized accumulation of [^{11}C]PBB3 in the medial temporal region of AD patients was accompanied by marked hippocampal atrophy (Figure 7B). Notably, [^{11}C]PBB3-PET signals were substantially increased, notwithstanding the atrophy-related partial volume effects on PET images, and this

observation may support the contribution of tau fibrils to toxic neuronal death in AD. However, these data do not immediately imply neurotoxicities of [^{11}C]PBB3-reactive tau fibrils, in light of MRI-detectable neurodegeneration uncoupled with [^{11}C]PBB3 retention in the hippocampus of PS19 mice. In the hippocampal formation of AD patients, neurons bearing NFTs that resemble those in the PS19 hippocampus may drive neurodegeneration similar to that observed in either the PS19 hippocampus or brain stem, and this issue could be addressed in future studies using [^{11}C]PBB3-PET and MRI in diverse mouse models, including PS19 and rTg4510 mice, and human subjects.

Our analyses of multiple β sheet ligands illustrated electrochemical and/or conformational diversities of β-pleated sheets among amyloid aggregates, producing a selectivity of these compounds for a certain spectrum of fibrillar pathologies (Figures 1 and S1). Lipophilicities of the β sheet ligands could determine their reactivity with noncored plaques, as noted among the PBBs studied here (Figure 1), although the molecular properties underlying this variation are yet to be elucidated. Meanwhile, we noted that all β sheet ligands tested in the present study were reactive with dense core plaques regardless of their lipophilicities. This may affect in vivo PET signals, particularly in AD brain areas with abundant cored plaques, such as the precuneus. However, our combined autoradiographic and histochemical assessments indicated that [^{11}C]PBB3 bound to dense core plaques accounts for less than 10% of total specific radioligand binding in these areas, and this percentage in fact includes binding to tau fibrils in plaque neurites in addition to Aβ amyloid core. A second possibility to account for the diversity of ligand reactivity to tau lesions may arise from the packing distance between two juxtaposed β sheets in tau filaments and is discussed in the Supplemental Discussion.

Notably, selectivity of [^{11}C]PBB3 for tau versus aggregates may depend on free radioligand concentration in the brain. Our autoradiographic binding assays suggested that affinity of [^{11}C]PBB3 for NFTs is 40- to 50-fold higher than senile plaques, but binding components on tau fibrils may be more readily saturated by this radioligand than those on Aβ fibrils. [^{11}C]PBB3-PET data in humans indicated that uptake of this radioligand into the brain is less than one-third of [^{11}C]PIB uptake and that free radioligand concentration in the brain at a pseudoequilibrium state is approximately 0.2 nM or lower. In this range of concentration, [^{11}C]PBB3 could preferentially interact with high-affinity binding components formed by tau assemblies. An excessive amount of radioligand in the brain would result in saturation of radioligand binding to tau lesions and increased binding to low-affinity, high-capacity binding components in Aβ plaques, and such overload of free radioligand is more likely in regions with less abundant tau pathologies. This could be even more critical in capturing early tau pathologies that originate in the hippocampal formation and may require technical improvements and methodological refinements, including high-resolution imaging, correction for motions of subjects during scans, and robust definition of VOIs on the atrophic hippocampus.

Although nonspecific [^{11}C]PBB3-PET signals in control human subjects were generally low, radioligand retention in dural venous sinuses was noticeable in all scanned individuals. Possible mechanisms that underlie this property are discussed in the Supplemental Discussion.

The present work has also implied the potential utility of multimodal imaging systems for translational development of therapeutic agents that counteract tau fibrillogenesis. Optical imaging with a near-infrared fluorescent probe, such as PBB5, could provide the least invasive technique to assess tau accumulation in living mouse models. As demonstrated by our in vitro and ex vivo fluorescence labeling, all PBBs share a similarity in terms of their reactivity with tau aggregates. Hence, PBB5 optics may be applicable to early screening of therapeutic agents that suppress tau deposition, and the data on abundance of tau lesions obtained by this approach may be translatable to advanced stages of assessments using [^{11}C]PBB3-PET in animal models and humans. By contrast, pharmacokinetic properties of PBB5 (Figure S5) were found to be distinct from those of electrically neutral PBBs, including PBB2 and PBB3. These considerations would be of importance in developing and using fluorescent ligands applicable to optical and PET imaging.

To conclude, our class of multimodal imaging agents offers the possibility of visual investigations of fibrillary tau pathologies at subcellular, cellular, and regional levels. These assay systems are potentially powerful tools for the longitudinal evaluation of anti-tau treatments (Marx, 2007), as a single probe may facilitate a seamless, bidirectional translation between preclinical and clinical insights. PET tracers would also serve a more immediate therapeutic purpose by enabling the assessment of the effects of anti-Aβ and anti-tau therapies on tau pathologies in living AD patients.

EXPERIMENTAL PROCEDURES

Compounds and Reagents

PBB1 (Wako Pure Chemical Industries), PBB2 (ABX), PBB3 (Nard Institute), PBB4 (ABX), mPBB5 (Nard Institute), desmethyl precursor of [^{11}C]PBB2 (2-[4-(4-aminophenyl)buta-1,3-dienyl]benzothiazol-6-ol; Nard Institute), desmethyl precursor of [^{11}C]PBB3 protected with a silyl group (5-[4-(6-tert-butyldimethylsilyloxy-benzothiazol-2-yl)buta-1,3-dienyl]pyridine-2-amine; Nard Institute), desmethyl precursor of [^{11}C]mPBB5 (2-[4-(4-dimethylaminophenyl) buta-1,3-dienyl]-3-ethyl-6-hydroxybenzothiazol-3-ium; Nard Institute), and 2-[8-(4-dimethylaminophenyl)octa-1,3,5,7-tetraenyl]-3-ethylbenzothiazol-3-ium (DM-POTEB; Nard Institute) were custom synthesized. Information on other chemicals is provided in the Supplemental Experimental Procedures. ClogP for each compound was calculated using ACD Chemsketch logP software (Advanced Chemistry Development).

Animal Models

Tg mice heterozygous for human T34 (4-repeat tau isoform with 1 N-terminal insert) with FTDP-17 P301S mutation driven by mouse prion protein promoter, also referred to as PS19 mice (Yoshiyama et al., 2007), were bred and kept on a C57BL/6 background. All mice studied here were maintained and handled in accordance with the National Research Council's Guide for the Care and Use of Laboratory Animals and our institutional guidelines. Protocols for the present animal experiments were approved by the Animal Ethics Committees of the National Institute of Radiological Sciences.

Postmortem Brain Tissues

Procedures for preparation of human and mouse brain sections are given in the Supplemental Experimental Procedures.

In Vitro and Ex Vivo Fluorescence Microscopy

Six micrometer paraffin sections generated from patient brains and 20 μm frozen sections of mouse brains were stained with 10^{-3}% β sheet ligands

dissolved in 50% ethanol for 1 hr at room temperature. Images of the fluorescence signals from these compounds were captured by nonlaser (BZ-9000; Keyence Japan) and confocal laser scanning (FV-1000; Olympus) microscopes. In the confocal imaging, excitation/emission wavelengths (nm) were optimized for each compound as follows: 405/420-520 (PBB3, FSB, PIB, BF-227, BF-158, FDDNP, thioflavin-S), 488/520-580 (PBB2, PBB4), 515/530-630 (PBB1, curcumin), and 635/645-720 (PBB5, BF-189, DM-POTEB). Subsequently, the tested samples and adjacent sections probed serially with each ligand were autoclaved for antigen retrieval, immunostained with the anti-tau monoclonal antibody AT8 that is specific for tau phosphorylated at Ser 202 and Thr 205 (Endogen), as well as a polyclonal antibody against Aβ N3(pE), and inspected using the microscopes noted above. For ex vivo imaging, PS19 and non-Tg WT at 10–12 months of age were anesthetized with 1.5% (v/v) isoflurane and were given 1 mg/kg PBB1-4, 0.1 mg/kg PBB5, or 10 mg/kg FSB by syringe via tail vein. The animals were killed by decapitation at 60 min after tracer administration. Brain and spinal cord were harvested and cut into 10-μm-thick sections on a cryostat (HM560). The sections were imaged using microscopes as in the in vitro assays and were labeled with either FSB or AT8, followed by microscopic re-examination.

Ex Vivo and In Vivo Multiphoton Imaging

Experimental procedures are given in the Supplemental Experimental Procedures.

In Vivo and Ex Vivo Pulsed Laser Scanning Imaging

Noninvasive scans of isoflurane-anesthetized non-Tg WT and tau Tg mice at 12 months of age were performed using a small animal-dedicated optical imager (eXplore Optix; ART). Scan protocols are given in the Supplemental Experimental Procedures.

Radiosynthesis of [^{11}C]PBB2

Experimental procedures are given in the Supplemental Experimental Procedures.

Radiosynthesis of [^{11}C]PBB3

[^{11}C]Methyl iodide was produced and transferred into 300 μl of dimethyl sulphoxide (DMSO) containing 1.5–2 mg of *tert*-butyldimethylsilyl desmethyl precursor and 10 mg of potassium hydroxide at room temperature. The reaction mixture was heated to 125°C and maintained for 5 min. After cooling the reaction vessel, 5 mg of *tetra-n*-butylammonium fluoride hydrate in 600 μl of water was added to the mixture to delete the protecting group, and then 500 μl of HPLC solvent was added to the reaction vessel. The radioactive mixture was transferred into a reservoir for HPLC purification (CAPCELL PAK C_{18} column, 10 × 250 mm; acetonitrile/50 mM ammonium formate = 4/6, 6 ml/min). The fraction corresponding to [^{11}C]PBB3 was collected in a flask containing 100 μl of 25% ascorbic acid solution and 75 μl of Tween 80 in 300 μl of ethanol and was evaporated to dryness under a vacuum. The residue was dissolved in 10 ml of saline (pH 7.4) to obtain [^{11}C]PBB3 (970–1,990 GBq at the end of synthesis [EOS]) as an injectable solution. The final formulated product was radiochemically pure (≥95%) as detected by analytic HPLC (CAPCELL PAK C_{18} column, 4.6 × 250 mm; acetonitrile/50 mM ammonium formate = 4/6, 2 ml/min). The specific activity of [^{11}C]PBB3 at EOS was 37–121 GBq/μmol, and [^{11}C]PBB3 maintained its radioactive purity exceeding 90% over 3 hr after formulation.

Radiosynthesis of [^{11}C]mPBB5

Experimental procedures are given as Supplemental Experimental Procedures.

Radiosynthesis of [^{11}C]PIB

Radiolabeling of PIB was performed as described elsewhere (Maeda et al., 2011). The specific activity of [^{11}C]PIB at EOS was 50–110 GBq/μmol.

In Vitro and Ex Vivo Autoradiography

Experimental procedures are given in the Supplemental Experimental Procedures.

In Vivo PET Imaging of Mice

PET scans were performed using a microPET Focus 220 animal scanner (Siemens Medical Solutions) immediately after intravenous injection of [^{11}C]PBB2 (28.3 ± 10.3 MBq), [^{11}C]PBB3 (29.7 ± 9.3 MBq), or [^{11}C]mPBB5 (32.8 ± 5.9 MBq). Detailed procedures are provided in the Supplemental Experimental Procedures.

In Vivo PET Imaging of Humans

Three cognitively normal control subjects (64, 72, and 75 years of age; mean age, 70.3 years) and three AD patients (64, 75 and 77 years of age; mean age, 72 years) were recruited to the present work (Figure 8). Additional information on these subjects is given in the Supplemental Experimental Procedures. The current clinical study was approved by the Ethics and Radiation Safety Committees of the National Institute of Radiological Sciences. Written informed consent was obtained from the subjects or their family members. PET assays were conducted with a Siemens ECAT EXACT HR+ scanner (CTI PET Systems). Detailed PET scan protocols are provided in the Supplemental Experimental Procedures. A fraction of radioactivity corresponding to unmetabolized [^{11}C]PBB3 in plasma at 3, 10, 20, 30, and 60 min was determined by HPLC (Waters mBondapak C_{18} column, 7.8 × 300 mm; acetonitrile/ammonium formate mobile phase with gradient elution = 40/60, 52/48, 80/20, 80/20, 40/60, and 40/60 at 0, 6, 7, 8, 9, and 15 min, respectively; flow rate, 6 ml/min) as described elsewhere (Suzuki et al., 1999). The radiotracer injection and following scans and plasma assays were conducted in a dimly lit condition to avoid photoracemization of the chemicals.

Individual MRI data were coregistered to the PET images using PMOD software (PMOD Technologies). Volumes of interest (VOIs) were drawn on coregistered MR images and were transferred to the PET images. Procedures of image analyses are provided in the Supplemental Experimental Procedures.

We additionally carried out PET scans of a patient who was clinically diagnosed as having corticobasal syndrome, as described in the Supplemental Experimental Procedures.

SUPPLEMENTAL INFORMATION

Supplemental Information includes Supplemental Experimental Procedures, nine figures, and one table and can be found with this article online at http://dx.doi.org/10.1016/j.neuron.2013.07.037.

ACKNOWLEDGMENTS

The authors thank Mr. T. Minamihisamatsu and Mr. Y. Matsuba for technical assistance, the staff of the Molecular Probe Group, National Institute of Radiological Sciences, for support with radiosynthesis, Dr. Y. Yoshiyama at National Hospital Organization Chiba-East Hospital for his support on clinical PET studies, and Dr. T. Iwatsubo at the University of Tokyo and Dr. H. Inoue at Kyoto University for their critical discussions. This work was supported in part by grants from the National Institute on Aging of the National Institutes of Health (AG10124 and AG17586) (to J.Q.T. and V. M.-Y.L.), Grants-in-Aid for Japan Advanced Molecular Imaging Program, Young Scientists (21791158) (to M.M.), Scientific Research (B) (23390235) (to M.H.), Core Research for Evolutional Science and Technology (to T.S.), Scientific Research on Innovative Areas ("Brain Environment") (23111009) (to M.H.) from the Ministry of Education, Culture, Sports, Science and Technology, Japan, Thomas H. Maren Junior Investigator Fund from College of Medicine, University of Florida (to N.S.), and research fund of Belfer Neurodegeneration Consortium (to Q.C. and M.-K.J.). M.M., H. Shimada, T.S., M.-R.Z., and M.H. are named as inventors on a patent application 0749006WO1, claiming subject matter related to the results described in this paper.

Accepted: July 12, 2013
Published: September 18, 2013

REFERENCES

Bacskai, B.J., Hickey, G.A., Skoch, J., Kajdasz, S.T., Wang, Y., Huang, G.F., Mathis, C.A., Klunk, W.E., and Hyman, B.T. (2003). Four-dimensional

multiphoton imaging of brain entry, amyloid binding, and clearance of an amyloid-β ligand in transgenic mice. Proc. Natl. Acad. Sci. USA *100*, 12462–12467.

Ballatore, C., Lee, V.M.Y., and Trojanowski, J.Q. (2007). Tau-mediated neurodegeneration in Alzheimer's disease and related disorders. Nat. Rev. Neurosci. *8*, 663–672.

Braak, H., and Braak, E. (1991). Neuropathological stageing of Alzheimer-related changes. Acta Neuropathol. *82*, 239–259.

Braak, H., Thal, D.R., Ghebremedhin, E., and Del Tredici, K. (2011). Stages of the pathologic process in Alzheimer disease: age categories from 1 to 100 years. J. Neuropathol. Exp. Neurol. *70*, 960–969.

Chien, D.T., Bahri, S., Szardenings, A.K., Walsh, J.C., Mu, F., Su, M.Y., Shankle, W.R., Elizarov, A., and Kolb, H.C. (2013). Early clinical PET imaging results with the novel PHF-tau radioligand [F-18]-T807. J. Alzheimers Dis. *34*, 457–468.

Dickson, D.W., Kouri, N., Murray, M.E., and Josephs, K.A. (2011). Neuropathology of frontotemporal lobar degeneration-tau (FTLD-tau). J. Mol. Neurosci. *45*, 384–389.

Engler, H., Forsberg, A., Almkvist, O., Blomquist, G., Larsson, E., Savitcheva, I., Wall, A., Ringheim, A., Långström, B., and Nordberg, A. (2006). Two-year follow-up of amyloid deposition in patients with Alzheimer's disease. Brain *129*, 2856–2866.

Fodero-Tavoletti, M.T., Okamura, N., Furumoto, S., Mulligan, R.S., Connor, A.R., McLean, C.A., Cao, D., Rigopoulos, A., Cartwright, G.A., O'Keefe, G., et al. (2011). ^{18}F-THK523: a novel *in vivo* tau imaging ligand for Alzheimer's disease. Brain *134*, 1089–1100.

Higuchi, M., Iwata, N., Matsuba, Y., Sato, K., Sasamoto, K., and Saido, T.C. (2005). ^{19}F and ^{1}H MRI detection of amyloid β plaques *in vivo*. Nat. Neurosci. *8*, 527–533.

Hintersteiner, M., Enz, A., Frey, P., Jaton, A.L., Kinzy, W., Kneuer, R., Neumann, U., Rudin, M., Staufenbiel, M., Stoeckli, M., et al. (2005). *In vivo* detection of amyloid-β deposits by near-infrared imaging using an oxazine-derivative probe. Nat. Biotechnol. *23*, 577–583.

Klunk, W.E., Wang, Y., Huang, G.F., Debnath, M.L., Holt, D.P., Shao, L., Hamilton, R.L., Ikonomovic, M.D., DeKosky, S.T., and Mathis, C.A. (2003). The binding of 2-(4′-methylaminophenyl)benzothiazole to postmortem brain homogenates is dominated by the amyloid component. J. Neurosci. *23*, 2086–2092.

Klunk, W.E., Engler, H., Nordberg, A., Wang, Y., Blomqvist, G., Holt, D.P., Bergström, M., Savitcheva, I., Huang, G.F., Estrada, S., et al. (2004). Imaging brain amyloid in Alzheimer's disease with Pittsburgh Compound-B. Ann. Neurol. *55*, 306–319.

Krebs, M.R.H., Bromley, E.H., and Donald, A.M. (2005). The binding of thioflavin-T to amyloid fibrils: localisation and implications. J. Struct. Biol. *149*, 30–37.

Kudo, Y., Okamura, N., Furumoto, S., Tashiro, M., Furukawa, K., Maruyama, M., Itoh, M., Iwata, R., Yanai, K., and Arai, H. (2007). 2-(2-[2-Dimethylaminothiazol-5-yl]ethenyl)-6- (2-[fluoro]ethoxy)benzoxazole: a novel PET agent for *in vivo* detection of dense amyloid plaques in Alzheimer's disease patients. J. Nucl. Med. *48*, 553–561.

Maeda, J., Ji, B., Irie, T., Tomiyama, T., Maruyama, M., Okauchi, T., Staufenbiel, M., Iwata, N., Ono, M., Saido, T.C., et al. (2007). Longitudinal, quantitative assessment of amyloid, neuroinflammation, and anti-amyloid treatment in a living mouse model of Alzheimer's disease enabled by positron emission tomography. J. Neurosci. *27*, 10957–10968.

Maeda, J., Zhang, M.R., Okauchi, T., Ji, B., Ono, M., Hattori, S., Kumata, K., Iwata, N., Saido, T.C., Trojanowski, J.Q., et al. (2011). *In vivo* positron emission tomographic imaging of glial responses to amyloid-beta and tau pathologies in mouse models of Alzheimer's disease and related disorders. J. Neurosci. *31*, 4720–4730.

Marx, J. (2007). Alzheimer's disease. A new take on tau. Science *316*, 1416–1417.

Okamura, N., Suemoto, T., Furumoto, S., Suzuki, M., Shimadzu, H., Akatsu, H., Yamamoto, T., Fujiwara, H., Nemoto, M., Maruyama, M., et al. (2005). Quinoline and benzimidazole derivatives: candidate probes for *in vivo* imaging of tau pathology in Alzheimer's disease. J. Neurosci. *25*, 10857–10862.

Santacruz, K., Lewis, J., Spires, T., Paulson, J., Kotilinek, L., Ingelsson, M., Guimaraes, A., DeTure, M., Ramsden, M., McGowan, E., et al. (2005). Tau suppression in a neurodegenerative mouse model improves memory function. Science *309*, 476–481.

Schmidt, M.L., Gur, R.E., Gur, R.C., and Trojanowski, J.Q. (1988). Intraneuronal and extracellular neurofibrillary tangles exhibit mutually exclusive cytoskeletal antigens. Ann. Neurol. *23*, 184–189.

Small, G.W., Kepe, V., Ercoli, L.M., Siddarth, P., Bookheimer, S.Y., Miller, K.J., Lavretsky, H., Burggren, A.C., Cole, G.M., Vinters, H.V., et al. (2006). PET of brain amyloid and tau in mild cognitive impairment. N. Engl. J. Med. *355*, 2652–2663.

Suzuki, K., Takei, M., and Kida, T. (1999). Development of an analyzing system for the sensitive measurement of radioactive metabolites on the PET study. J. Labelled Comp. Radiopharm. *42*, S658–S660.

Thompson, P.W., Ye, L., Morgenstern, J.L., Sue, L., Beach, T.G., Judd, D.J., Shipley, N.J., Libri, V., and Lockhart, A. (2009). Interaction of the amyloid imaging tracer FDDNP with hallmark Alzheimer's disease pathologies. J. Neurochem. *109*, 623–630.

Yang, L., Rieves, D., and Ganley, C. (2012). Brain amyloid imaging—FDA approval of florbetapir F18 injection. N. Engl. J. Med. *367*, 885–887.

Yoshiyama, Y., Higuchi, M., Zhang, B., Huang, S.M., Iwata, N., Saido, T.C., Maeda, J., Suhara, T., Trojanowski, J.Q., and Lee, V.M.Y. (2007). Synapse loss and microglial activation precede tangles in a P301S tauopathy mouse model. Neuron *53*, 337–351.

Zhang, W., Arteaga, J., Cashion, D.K., Chen, G., Gangadharmath, U., Gomez, L.F., Kasi, D., Lam, C., Liang, Q., Liu, C., et al. (2012). A highly selective and specific PET tracer for imaging of tau pathologies. J. Alzheimers Dis. *31*, 601–612.

Zhuang, Z.P., Kung, M.P., Hou, C., Skovronsky, D.M., Gur, T.L., Plössl, K., Trojanowski, J.Q., Lee, V.M.Y., and Kung, H.F. (2001). Radioiodinated styrylbenzenes and thioflavins as probes for amyloid aggregates. J. Med. Chem. *44*, 1905–1914.

EXHIBIT 80

FierceDiagnostics

Published on FierceDiagnostics (http://www.fiercediagnostics.com)

Alzheimer's diagnosis may gain from PET imaging of tau proteins

September 20, 2013 | By Mark Hollmer

An international group of researchers from Japan and the U.S. say they've developed a way to use PET imaging to diagnose Alzheimer's in a living person and then track the disease's advance. The key: an imaging agent drawn to the buildup of tau protein in the brain.

Forbes, the *BBC* and other news outlets picked up on this major advance, which, if supported by future research, could improve how patients are both diagnosed and treated for Alzheimer's. The journal *Neuron* carries the full study and its findings.

Right now, the only way to definitively diagnose Alzheimer's is through an autopsy. A number of companies are advancing imaging agents that would help, in theory, to diagnose the disease in living patients. Navidea ($NAVB) is underway with a Phase III trial of an imaging agent that can detect beta-amyloid deposits in the brain--the compound can be a telltale sign of Alzheimer's. GE Healthcare also has an investigative imaging agent that tracks beta-amyloid, and it has done well in Phase III. Both trigger vivid images through PET scans.

As *Forbes* explains, this new study differed because it relied on a fluorescent material drawn to tau protein, thought to be another sign of Alzheimer's or budding dementia. The substance crossed the blood brain barrier and worked in both mice and several human patients. And as the *BBC* notes, those tags, combined with positron emission tomography, helped build a three-dimensional image of tau buildup in the brain that clinicians haven't had before.

These are early results, of course. But if further research can duplicate these findings, then doctors get a new way to potentially track and diagnose the disease. The advance could also give researchers a tool to test Alzheimer's drugs by tracking how the tau protein buildup responds to a given treatment through detailed PET scans. What's more, detailed imaging could lead to earlier diagnosis and treatment, which doctors believe may be the best way to slow Alzheimer's advance.

- here's the *Forbes* story
- check out the *BBC*'s take
- here's the journal abstract

Related Articles:
Navidea keys up Alzheimer's Dx agent for Phase III
GE touts promising PhIII for Alzheimer's imaging agent
GE Healthcare joins Australian government on Alzheimer's Dx study

Source URL: http://www.fiercediagnostics.com/story/alzheimers-diagnosis-may-gain-pet-imaging-tau-proteins/2013-09-20

EXHIBIT 81

BRAIN
A JOURNAL OF NEUROLOGY

SCIENTIFIC COMMENTARIES

Time for tau

It is almost exactly 10 years since the first report of a PET ligand that specifically bound to a pathological protein in the brain was published (Klunk *et al*., 2004). This tracer, ^{11}C-Pittsburgh compound B (PIB), detected fibrillar aggregated forms of amyloid-β, the major constituent of the Alzheimer's disease plaque and, according to many, the initiating event in Alzheimer's disease pathogenesis. This report was soon followed by several amyloid imaging tracers that were radiolabelled with the longer half-life positron-emitting nuclide ^{18}F, opening the door to commercial manufacture and clinical application. Several of these tracers are now approved by worldwide regulatory agencies including the US Food and Drug Administration and the European Medicines Agency, although reimbursement for clinical use remains problematic. In this issue of *Brain*, Okamura and colleagues report the first human PET studies with a new tracer for tau, ^{18}F-THK5105, and reveal that retention of this tracer correlates with dementia severity and brain atrophy in Alzheimer's disease (Okamura *et al*., 2014).

Because it is difficult to develop, test and validate a new PET imaging agent, it may have seemed overly optimistic 10 years ago to conclude that a new era in human brain imaging had begun, but it had. The latest developments are a series of PET tracers that bind to the microtubule-associated protein tau that is aggregated as neurofibrillary tangles in Alzheimer's disease. Tau-related diseases also include the group of tauopathies often referred to as frontotemporal lobar degenerations, and the highly publicized chronic traumatic encephalopathy. Tau would seem to be a difficult target for PET imaging: it may be intracellular thus requiring tracer passage across both the blood–brain barrier and cell membranes; it is found in the brain at lower concentrations than amyloid-β; and it is characterized by different isoforms reflecting alternative splicing with either three (3R) or four (4R) repeated microtubule binding domains. The first PET tau imaging agent to be reported, ^{18}F-FDDNP, was not specific for tau and showed relatively low uptake. However, in the past few years, three research groups have investigated separate molecular structures resulting in three series of compounds that are promising tau-binding PET tracers. One of these, ^{11}C-PBB3 (Maruyama *et al*., 2013), has shown *in vitro* binding to tau in the form of neurofibrillary tangles, neuropil threads and plaque neurites in Alzheimer's disease brain tissue, and also *in vitro* binding to tau inclusions in tissue from patients with Pick's disease (a 3R tauopathy), or progressive supranuclear palsy and corticobasal degeneration (4R tauopathies). PET studies showed hippocampal uptake in cognitively normal older people, and extensive cortical binding in patients with Alzheimer's disease that appeared largely consistent with the pathological staging proposed by Braak and Braak (1991). Another series of compounds includes the ^{18}F-labelled T807 and T808 (Chien *et al*., 2013, 2014); these compounds both demonstrate tau binding to Alzheimer's disease brain tissue without labelling amyloid-β. They show good *in vivo* brain penetration in humans and patterns of retention on PET scans that again are consistent with Braak staging.

The third group of ^{18}F-labelled compounds comprises the 'THK' series developed at Tohoku University. The first of this series, ^{18}F-THK523, was reported by Fodero-Tavoletti *et al*. (2011), and although tissue studies indicated good selectivity for tau over amyloid-β, subsequent human PET experiments showed low cortical binding compared to binding in white matter, making signal detection difficult. Okamura and colleagues now report the first human PET studies of the related compound ^{18}F-THK5105 (Okamura *et al*., 2014). They studied eight patients with Alzheimer's disease and eight older control subjects with ^{18}F-THK5105 and ^{11}C-PIB. ^{18}F-THK5105 data acquired over 2 h showed that tracer activity in the cerebellar cortex washed out similarly in patients and control subjects, whereas tracer retention occurred in the temporal lobe in patients with Alzheimer's disease. By 90 min post-injection, ratios in cortex to cerebellum averaged 1.32 in the inferior temporal lobe of patients (the neocortical region with highest retention) compared with 1.09 in control subjects. Although other cortical regions generally showed higher retention in patients than controls, the highest brain signal was seen in pons, and this was similar in both patients and control subjects. Other subcortical brain regions showing high uptake included putamen and white matter, which did not differ between patients and control subjects. In controls, tracer retention in medial temporal regions was higher than in neocortex, suggesting the presence of medial temporal lobe neurofibrillary tangles, a common finding in ageing. ^{11}C-PIB uptake revealed a very different pattern, with highest uptake in precuneus and frontal cortex; uptake of the two tracers was not statistically correlated. In addition, associations were found between ^{18}F-THK5105 retention and both cognitive and magnetic resonance volumetric measures that were not seen with ^{11}C-PIB.

These data are very supportive of the use of ^{18}F-THK5105 in the study of Alzheimer's disease, with a number of important potential applications. Okamura *et al.* (2014) note that

^{18}F-THK5105 retention in the inferior temporal cortex showed no overlap between patients and control subjects, suggesting that tau imaging could be diagnostically useful, although the samples are still quite small. Reports that the related compound THK523 did not bind to tau deposited in the tauopathies of corticobasal degeneration, progressive supranuclear palsy, and Pick's disease (Fodero-Tavoletti *et al*., 2014) may be good news if we are looking for a disease-specific biomarker, but bad news if we are looking for a biomarker to image frontotemporal lobar degeneration syndromes. The findings that brain ^{18}F-THK5105 paralleled both clinical measures of severity and magnetic resonance measures of atrophy, though preliminary, are consistent with observations that post-mortem measures of neurofibrillary tangle pathology are among the best correlates of disease severity in patients with Alzheimer's disease and suggest that tau imaging could be a staging method that might also be useful in detecting response to a therapeutic agent. Recent attempts to develop PET amyloid imaging as surrogate markers of treatment efficacy have been disappointing in failing to show either a strong relationship with dementia severity or prediction of clinical therapeutic response (Salloway *et al*., 2014). Because tau pathology correlates with symptoms, tau imaging could be a potential surrogate outcome for any therapy that has clinical benefit and would certainly be a useful biomarker in a trial of a therapeutic agent targeted to tau itself, an especially important goal in relation to frontotemporal lobar degeneration.

In addition to potential applications to clinical trials, tau imaging will be of major benefit for understanding the pathological progression of Alzheimer's disease and differentiating it from normal ageing. Current models of Alzheimer's disease are problematic in many respects, one of which is the difficulty in defining the relative importance of neurodegeneration as opposed to amyloid-β deposition. Although early models of biomarker change in Alzheimer's disease posited that amyloid-β was an initiating event, evidence of neurodegeneration in the absence of amyloid-β has resulted in a pathological framework that admits the possibility of independent and early tauopathy in Alzheimer's disease (Jack *et al*., 2013). The suggestion that all of the tau imaging agents are retained in the medial temporal lobes of older control subjects offers the promise that the relationship between medial temporal tau and neocortical amyloid-β can be disentangled, as well as the relationships between both of these proteins and brain atrophy, hypometabolism and cognition.

We now have at least three distinct ligands for human tau imaging. PET imaging of neurodegenerative diseases is rapidly evolving and there will undoubtedly be new tau imaging agents on the way, along with additional agents for other proteins such as α-synuclein. In fact, Okamura *et al*. (2014) note that they have developed another related compound, ^{18}F-THK5117, which has more favourable pharmacokinetic and binding properties. There are no data for comparison of the THK series compounds with ^{18}F-T807 and ^{11}C-PBB3, although the ^{11}C label of PBB3 will limit its use to institutions with PET radiochemistry programs unless an ^{18}F label can be developed. Which of these compounds is 'best' is a complex determination that will have to be defined by the intended use and additional data that accrue in this rapidly developing field. No PET ligand is perfect, and these tau ligands are likely to differ by specificity (do they bind to different forms of tau and to non-tau targets?), sensitivity (how much tau signal can be detected compared to non-specific background binding?), pharmacokinetics (is brain penetration high and steady state achieved early enough to yield good images?) and other factors. The implications for understanding Alzheimer's disease and developing effective treatments are important, and as we learn more about the behaviour of different ligands we may open up new avenues to the study of non-Alzheimer's disease tauopathies and chronic traumatic encephalopathy. The pace of scientific discovery is accelerating and the end result will be more tools and more information that should result in more effective treatments.

William Jagust
University of California Berkeley, USA

Correspondence to: William Jagust
E-mail: jagust@berkeley.edu

Advance Access publication April 15, 2014
doi:10.1093/brain/awu093

References

Braak H, Braak E. Neuropathological staging of Alzheimer-related changes. Acta Neuropathol 1991; 82: 239–59.

Chien DT, Bahri S, Szardenings AK, Walsh JC, Mu F, Su MY, et al. Early clinical PET imaging results with the novel PHF-tau radioligand [F-18]-T807. J Alzheimers Dis 2013; 34: 457–68.

Chien DT, Szardenings AK, Bahri S, Walsh JC, Mu F, Xia C, et al. Early clinical PET imaging results with the novel PHF-tau radioligand [F18]-T808. J Alzheimers Dis 2014; 38: 171–84.

Fodero-Tavoletti MT, Furumoto S, Taylor L, McLean CA, Mulligan RS, Birchall I, et al. Assessing THK523 selectivity for tau deposits in Alzheimer's disease and non Alzheimer's disease tauopathies. Alzheimers Res Ther 2014; 6: 11.

Fodero-Tavoletti MT, Okamura N, Furumoto S, Mulligan RS, Connor AR, McLean CA, et al. 18F-THK523: a novel *in vivo* tau imaging ligand for Alzheimer's disease. Brain 2011; 134 (Pt 4): 1089–100.

Jack CR Jr, Knopman DS, Jagust WJ, Petersen RC, Weiner MW, Aisen PS, et al. Tracking pathophysiological processes in Alzheimer's disease: an updated hypothetical model of dynamic biomarkers. Lancet Neurol 2013; 12: 207–16.

Klunk WE, Engler H, Nordberg A, Wang Y, Blomqvist G, Holt DP, et al. Imaging brain amyloid in Alzheimer's disease with Pittsburgh Compound-B. Ann Neurol 2004; 55: 306–19.

Maruyama M, Shimada H, Suhara T, Shinotoh H, Ji B, Maeda J, et al. Imaging of tau pathology in a tauopathy mouse model and in Alzheimer patients compared to normal controls. Neuron 2013; 79: 1094–108.

Okamura N, Furumoto S, Fodero-Tavoletti M, Mulligan RS, Harada R, Yates P, et al. Noninvasive assessment of Alzheimer's disease neurofibrillary pathology using ^{18}F-THK-5101 PET. Brain 2014in press.

Salloway S, Sperling R, Fox NC, Blennow K, Klunk W, Raskind M, et al. Two phase 3 trials of bapineuzumab in mild-to-moderate Alzheimer's disease. N Engl J Med 2014; 370: 322–33.

EXHIBIT 82

McGRATH: Illinois Eye Institute project aims to identify CTE in the living

BY DAN MCGRATH For Sun-Times Media June 14, 2014 4:35PM

Updated: June 14, 2014 4:39PM

David Diaz knows he probably should have told someone about the double vision he experienced near the end of his world-class boxing career, but the disclosure would have cost him the thing that defined him and enabled him to provide for his family.

Fighters fight, and Diaz — a U.S. Olympian at 20 in 1996 and a crowd-pleasing world lightweight champion 10 years later — was a fighter's fighter.

''It was worst when I looked at somebody straight-on,'' he recalled. ''In the ring, you're always moving your head, so I could adapt.''

Diaz spent two years and four fights trying to regain the title he lost to Manny Pacquiao in a brutal ninth-round stoppage that showed ''PacMan'' at the peak of his relentless powers and left Diaz looking as though he had been in a knife fight. He decided he'd had enough and retired in 2011, after a sneaky right hand from Philadelphia prospect Hank Lundy sliced open his right eyebrow and drew a river of blood from the worst cut of his 41-bout pro career.

''I didn't see it coming,'' Diaz said.

A boxer who can't see punches coming had best seek a new line of work. Diaz also wanted to be a husband to his wife, Tonya, and a father to their boys, David, Elias and Silas.

A consultation with Dr. Robert Steinmetz led to corrective treatment for Diaz's double vision. Steinmetz, a Chicago optometrist and former college baseball player whose wife, Nicole, was a Golden Gloves boxing champion, also persuaded Diaz to participate in a research project the Illinois Eye Institute is conducting to examine whether irregularities in the vision, movements and retina/optic nerve structure in the eyes of contact-sport participants might be a marker for the tau protein that causes chronic traumatic encephalopathy (CTE) in concussed athletes.

CTE, brought on by multiple concussions, accelerates deterioration of the brain and has been cited as a factor in the deaths of several high-profile former football players, including Pittsburgh Steelers great Mike Webster and former Bears safety Dave Duerson.

''One thing that's known about CTE is it's related to the number of times you get hit in the head,'' said Dr. Leonard Messner, who is directing the project as executive director of the institute. ''A concussion is a metabolic change within the brain, more of a biomechanical injury than structural. Eighty to 85 percent of them go unreported.''

With that in mind, Messner is working with the Chicago Concussion Coalition to standardize screening procedures so concussed athletes are identified more readily and removed from harm's way. They're part of a National Hit Count Initiative designed to track how often athletes are exposed to potentially damaging collisions. And they have persuaded the Illinois High School Association to ban full-contact football drills during the offseason.

''The biggest risk factor in sustaining a concussion is having had one previously,'' Messner said, ''and 'return to play' guidelines are purely speculative.''

The Illinois project is affiliated with the Sports Legacy Institute, the Boston University-based group that has pioneered CTE research through the work of neurosurgeons Ann McKee and Robert Cantu and the tireless awareness-raising of *Head Games* author Chris Nowinski, a college football star/professional wrestler/concussion victim.

On Wednesday at the Union League Club, the Sports Legacy Institute will honor former Bears quarterback Jim McMahon for his courage in coming forward as a possible CTE case. McMahon has acknowledged experiencing memory loss, severe headaches, blurred vision and other symptoms of post-concussion syndrome.

To date, the only method of identifying CTE is through post-mortem examination of the brains of suspected victims. Researchers are

working to detect its presence in the living, before the deterioration of the brain begins.

Dr. Messner's group has tested more than 30 former football players, boxers and hockey players.

''It's a macho thing with boxers to say they've never been knocked out, so they'll tell us they've never had a concussion,'' Dr. Steinmetz said. ''But you don't have to be knocked out to have a concussion.''

Diaz knows.

''I've had multiple,'' he said.

And though his eye-test results were in the ''normal'' range, he limits his boxing activity to working with a youth group in Cicero.

''I hold the mitts for them, teach them footwork,'' he said. ''They all want to spar, but I won't get in the ring with them. If I did, I might be tempted, start thinking, 'I can still do this.' But I won't. Not many of us walk away clean. I want to be there for my kids.''